Title
Epstein-Barr Virus Transcytosis through Polarized Oral Epithelial Cells

Journal
Journal of Virology, 87(14)

ISSN
0022-538X

Authors
Tugizov, Sharof M
Herrera, Rossana
Palefsky, Joel M

Publication Date
2013-07-15

DOI
10.1128/jvi.00443-13

Peer reviewed

JVI Journals.ASM.org

Epstein-Barr Virus Transcytosis through Polarized Oral Epithelial Cells

Sharof M. Tugizov,[a,b] Rossana Herrera,[a] Joel M. Palefsky[a,b]

Department of Medicine[a] and Department of Orofacial Sciences,[b] University of California San Francisco, San Francisco, California, USA

Although Epstein-Barr virus (EBV) is an orally transmitted virus, viral transmission through the oropharyngeal mucosal epithelium is not well understood. In this study, we investigated how EBV traverses polarized human oral epithelial cells without causing productive infection. We found that EBV may be transcytosed through oral epithelial cells bidirectionally, from both the apical to the basolateral membranes and the basolateral to the apical membranes. Apical to basolateral EBV transcytosis was substantially reduced by amiloride, an inhibitor of macropinocytosis. Electron microscopy showed that virions were surrounded by apical surface protrusions and that virus was present in subapical vesicles. Inactivation of signaling molecules critical for macropinocytosis, including phosphatidylinositol 3-kinases, myosin light-chain kinase, Ras-related C3 botulinum toxin substrate 1, p21-activated kinase 1, ADP-ribosylation factor 6, and cell division control protein 42 homolog, led to significant reduction in EBV apical to basolateral transcytosis. In contrast, basolateral to apical EBV transcytosis was substantially reduced by nystatin, an inhibitor of caveolin-mediated virus entry. Caveolae were detected in the basolateral membranes of polarized human oral epithelial cells, and virions were detected in caveosome-like endosomes. Methyl β-cyclodextrin, an inhibitor of caveola formation, reduced EBV basolateral entry. EBV virions transcytosed in either direction were able to infect B lymphocytes. Together, these data show that EBV transmigrates across oral epithelial cells by (i) apical to basolateral transcytosis, potentially contributing to initial EBV penetration that leads to systemic infection, and (ii) basolateral to apical transcytosis, which may enable EBV secretion into saliva in EBV-infected individuals.

Epstein-Barr virus (EBV) is an oncogenic human herpesvirus causing tumors in B lymphocytes (Burkitt's lymphoma and Hodgkin's disease) and epithelial cells (nasopharyngeal and gastric carcinoma). Worldwide, about 200,000 new cases of EBV-associated cancer are reported each year. The tissue tropism of EBV *in vivo* is mainly restricted to B lymphocytes and epithelial cells. Virus infection in B lymphocytes is mainly latent, whereas in epithelial cells, it is lytic, i.e., productive (1).

EBV infection in B lymphocytes and epithelial cells is initiated by attachment of virions to the cell surface (2, 3). In B lymphocytes, the EBV glycoprotein gp350/220 plays an important role in virus attachment through binding to the cell surface receptor CD21. Virus entry occurs by endocytosis and subsequent fusion of viral and endosomal membranes, which is mediated by the EBV glycoproteins gHgL, gB, and gp42 (4–8). EBV entry into nonpolarized epithelial cells does not require endocytosis of virions, and this process is likely initiated by direct fusion of viral and cell membranes (9, 10). EBV gHgL interacts with αv family integrins in epithelial cells, leading to the fusion of viral and cell membranes (11, 12). EBV gp350/220 and gp42 may not be required for EBV infection of epithelial cells, in contrast to gHgL and gB, which are essential for virus entry into epithelial cells (2, 8, 9, 13–17). EBV BMRF-2 interactions with β1 and αv family integrins are critical for infection and spread of virus in polarized oropharyngeal epithelial cells (18–21).

The oropharyngeal mucosal epithelium is a portal for viral entry in primary EBV infection (22–27). Abundant secretion of EBV virions into saliva by EBV-seropositive individuals is well documented (28–32), suggesting that the oral epithelium may also play a role in EBV release into saliva and transmission to others.

The oropharyngeal epithelium consists of multiple layers of stratified squamous epithelial cells supported by an underlying layer of fibrous connective tissue, the lamina propria (33). It has been shown that stratified mucosal epithelia, including the oral mucosal epithelium, have well-developed tight junctions (34–37), which initiate development of the distinct polarized apical and basolateral membranes of epithelial cells (38, 39). The polarization of epithelial cells determines the pathways of viral entry and egress (18, 39–48). The apical surfaces of monostratified polarized oral epithelial cells and *ex vivo* multistratified oral epithelium are not highly susceptible to cell-free EBV entry and productive infection (18, 49, 50). However, cell-free EBV does enter polarized oral epithelial cells from their basolateral membranes, leading to productive infection (18, 49).

It is well documented that polarized tonsil, endometrial, liver, placental, kidney, and intestinal epithelial cells facilitate rapid transcellular transcytosis of various human viruses, including human immunodeficiency virus (HIV), human cytomegalovirus (HCMV), influenza virus, and poliovirus (38, 39, 51–59). Transcytosis of viruses may occur bidirectionally (41, 60), i.e., from both the apical to the basolateral membranes and the basolateral to the apical membranes, and do so by the following sequential steps: (i) endocytosis of virions into early endosomal and sorting vesicles, (ii) sorting and delivery of virions to basolateral (or apical) vesicles, and (iii) release of virions from the basolateral (or apical) membranes. Viral transcytosis may lead to transport of virions from one membrane to the opposite membrane through the cytoplasm without infecting cells.

Received 12 February 2013 **Accepted** 29 April 2013
Published ahead of print 22 May 2013
Address correspondence to Sharof M. Tugizov, sharof.tugizov@ucsf.edu.

doi:10.1128/JVI.00443-13

EBV transcytosis across polarized epithelial cells of the kidneys and liver has been reported previously (53). Since oropharyngeal epithelium is critical for EBV entry and spread, we investigated transcytosis of EBV in polarized human oral epithelial cells. We found that EBV transcytosis in oral epithelial cells may occur bidirectionally, from both the apical to the basolateral membranes and the basolateral to the apical membranes, with different mechanisms used for each direction. Apical to basolateral EBV transcytosis was mediated by macropinocytosis, whereas basolateral to apical transcytosis was mediated by caveolin-mediated and caveosomal endocytosis.

MATERIALS AND METHODS

Ethics statement. This study was conducted according to the principles expressed in the Declaration of Helsinki. The study was approved by the Committee on Human Research of the University of California San Francisco (IRB approval number H8597-30664-03). All subjects provided written informed consent for the collection of tissue and serum samples.

Cells and virus. Palatine tonsil tissues used for the propagation of primary tonsil keratinocytes were obtained from 8 independent donors and provided by the National Disease Research Interchange (NDRI). Tonsil keratinocytes were propagated as described in our previous work (39). The purity of epithelial cells was determined by detection of keratins using a cocktail of antikeratin antibodies containing Ab-1 and Ab-2 (Thermo Scientific), and only those epithelial cell populations that were 100% positive for keratin were used. PCR analysis showed that all of these keratinocytes were negative for EBV.

Polarized cells were established in Transwell two-chamber filter inserts (0.4-μm pore size, 12-well inserts) as described in our previous work (18, 48). The polarity of epithelial cells was verified by confocal immunofluorescence of the tight junction proteins ZO-1 and occludin and measurement of paracellular permeability and transepithelial resistance (TER), as described previously (18, 39, 47, 48). Briefly, TER was measured with an epithelial Millicell-ERS voltohmmeter (Millipore). Paracellular permeability was evaluated by adding horseradish peroxidase-conjugated goat anti-donkey IgG $(Fab)_2$ (Jackson ImmunoResearch) to the upper filter compartment and photometrically assaying the medium from the lower compartment for horseradish peroxidase with *o*-phenylenediamine dihydrochloride as the substrate (61). Detection of IgG in the lower chamber indicated leakage of IgG from the upper chamber. Polarized cells showing leakage using this assay were not used. The bidirectional EBV transcytosis assay was established as described in Results.

An EBV B95-8-producing marmoset B-lymphoblastoid cell line and EBV Akata-infected Burkitt's lymphoma cells were maintained in RPMI 1640 medium supplemented with 10% fetal calf serum. For propagation of viral stocks, B95-8 cells were treated with 30 ng/ml of 12-*O*-tetradecanoyl phorbol 12-myristate 13-acetate (PMA) and 4 mM butyric acid (both from Sigma) in the growth medium for 10 days. Production of Akata EBV was induced with anti-IgG (DakoCytomation) as described previously (62). Virus-containing media were cleared of cell debris by centrifugation at 5,000 × *g* for 15 min, followed by filtration of the supernatant first through 0.8-μm-pore-size filters and then through 0.45-μm-pore-size filters (Millipore). Virus was concentrated by high-speed centrifugation, and the viral pellet was resuspended in RPMI 1640 medium. To quantify the encapsidated DNA, 10 μl of viral sample was treated with 2 μl of DNase I (105 U/ml) for 1 h, and DNase was inactivated at 90°C for 10 min (63). The viral titer was determined by quantitative real-time PCR (qPCR) as described in our previous work (20, 21).

For inactivation of EBV by UV light, B95-8 virus-containing culture medium in an uncovered plastic petri dish (60-mm diameter) sitting in an ice bath was exposed to UV light (1,200 J/cm^2) for 10 min in a CL-1000 UV cross-linker (UVP) (64).

Treatment of polarized cells with pharmacological agents. To inhibit EBV endocytosis and transcytosis, polarized cells were pretreated with pharmacological inhibitors. First, we determined the nontoxic concentrations of inhibitors in polarized tonsil epithelial cells using a 3-(4,5-dimethyl-2-thiazolyl)-2,5-diphenyl-2H-tetrazolium bromide (MTT) assay (Biotium Inc.). Polarized cells were pretreated for 1 h with nontoxic concentrations of chlorpromazine (20 μM), nystatin (12.5 μg/ml), 5-(*N*-ethyl-*N*-isopropyl)amiloride (20 to 100 μM), LY294002 (100 μM), rottlerin (100 μM), dynasore (40 μM), and ML9 (10 μM) (all from Sigma). All drug treatments were performed at both apical and basolateral membranes of polarized cells. After drug treatment, cells were washed and used for transcytosis assays. EBV was added to the upper chambers of inserts with apically and basolaterally oriented cells. After 4 h, basolateral media containing virus were collected and used for qPCR assay.

To determine the effect of drugs on virus attachment, cells were pretreated with chlorpromazine, nystatin, or amiloride for 1 h. Untreated cells served as a control. EBV B95-8 was added to the apical or basolateral membranes for 2 h at 4°C. Cells were washed twice with cold phosphate-buffered saline (PBS), pH 7.2, and cell extracts were prepared with cell lysis solution (5 Prime). One set of untreated cells was trypsinized to remove cell-bound virions (38, 65). EBV binding was quantitated by qPCR.

Treatment of EBV with antiviral human sera. Prior to transcytosis assays, EBV virions were preincubated with a pool of 4 human serum samples (AS-1, AS-2, AS-3, and AS-4) collected from healthy EBV-positive patients (66). These serum samples have anti-EBV VCA antibodies and neutralizing activity (66). As a control, a pool of 2 EBV-negative sera was used. EBV-negative human sera were purchased from Blackhawk BioSystems, Inc., and Wampole Laboratories. Virus-containing media were diluted with EBV-positive or -negative sera at 1:25, 1:50, and 1:100 and incubated at 37°C for 1 h. These virions were then used for apical to basolateral or basolateral to apical transcytosis assays.

Domain-specific cholesterol depletion in apical and basolateral membranes of polarized cells and its effect on EBV entry. For domain-specific cholesterol depletion, polarized cells were treated with 10 mM methyl β-cyclodextrin (MβCD) (Sigma) for 15 min at apical and/or basolateral membranes as described previously (67). Culture media were collected separately from the upper and lower chambers, and release of membrane cholesterol into culture media was measured using the Amplex red cholesterol assay kit (Life Technologies). After cholesterol depletion, cells were used for EBV entry assays. Cells were incubated with virus added to apical membranes for 1 h at 37°C, and TER was measured. Cells were then trypsinized with 0.25% trypsin (Sigma) and collected for qPCR analysis. Since trypsin removes cell-bound virions, the qPCR assay would detect only virions that had penetrated.

Transfection of cells with siRNAs. The following small interfering RNAs (siRNAs) were purchased from Santa Cruz Biotechnology Inc.: caveolin-1 (sc-29241), clathrin heavy chain (sc-35057), cell division control protein 42 homolog (Cdc42; sc-29256), Rac-1 (sc-36351), Pak1 (sc-29700), ARF6 (sc-43619), and dynamin 1/2 (sc-43736). As controls, unrelated (scrambled) siRNAs (sc-37007) were used (Santa Cruz Biotechnology Inc.). Polarized cells were transfected with siRNAs using lipid-based transfection reagents as described previously (39, 68). The efficiency of siRNA transfection was confirmed using fluorescein isothiocyanate (FITC)-labeled control siRNA; after 24 h, about 70 to 95% of the cells were positive for siRNA-FITC. Silencing of genes of interest by siRNAs at 48 h posttransfection was confirmed using a Western blot assay with antibodies to caveolin-1, clathrin, Cdc42, ARF6, and dynamin 2 (all from Abcam) and Rac-1 (Santa Cruz Biotech). Polarized cells were extracted, and proteins were separated on 16% SDS-polyacrylamide gels and immunoblotted with appropriate antibodies. Protein bands were visualized using enhanced chemiluminescence detection reagents (Amersham), and equal protein loading was confirmed by detection of β-actin (Ambion). Protein expression was quantitated by measuring the intensity of pixels (mean density) in protein bands using ImageJ software.

Confocal immunofluorescence microscopy. For immunofluorescence assays, cells were washed with PBS (pH 7.2), fixed with 4% parafor-

maldehyde and 2% sucrose in PBS for 5 min, and then permeabilized with 0.01% Triton X-100 in 4% paraformaldehyde for 5 min. The EBV viral capsid protein p18 was detected with goat anti-p18 antibody (Thermo Scientific). For colocalization of EBV p18 with markers of clathrin and caveolin, cells were exposed to EBV and costained with antibodies to clathrin and caveolin-1 (both from Abcam). Cells were examined by confocal microscopy (Bio-Rad MRC2400).

Determination of EBV copy numbers using a qPCR assay. Total DNA was extracted from culture media using an Archive Pure DNA Cell/Tissue kit (5 Prime). For qPCR assays (69), 20 ng of DNA was used for amplification of the EBV BZLF1 gene (specific primers: forward, 5′-AAA TTT AAG AGA TCC TCG TGT AA ACA TC-3′; reverse, 5′-CGC CTC CTG TTG CCG CAG AT-3′) and fluorogenic probe {5′ (6-carboxyfluorescein [FAM]) ATA ATG GAG TCA ACA TCC AGG CTT GGG C (6-carboxytetramethylrhodamine [TAMRA])-3′}. qPCR analysis was performed using an AB Prism 7900 detection system (Applied Biosystems). Thermocycling conditions were as follows: 50°C for 2 min, 95°C for 10 min, 95°C for 15 s, and 60°C for 1 min for 40 cycles. Each reaction mixture contained 1× TaqMan universal master mix with final concentrations of 5.5 mM $MgCl_2$, 200 μM deoxynucleoside triphosphates (dNTPs), 20 pmol each of forward and reverse primers, 10 pmol of TaqMan probe, and 0.5 U of Hotstart AmpliTaq Gold (Applied Biosystems) in a 20-μl volume in a 384-well plate. Experimental samples were run in quadruplicate, and the mean viral load was calculated. Each run had at least two "no template" controls to check for amplicon contamination. DNA from the Namalwa cell line (American Type Culture Collection), which contains two copies of EBV per cell, was used to generate standard curves (69).

EBV infectivity assay after viral transcytosis. Infectivity of transcytosed EBV was examined in freshly isolated $CD19^+$ B lymphocytes, which were purified from peripheral blood buffy coats (Pacifica Blood Center) as described in our previous work (50). Peripheral blood mononuclear cells (PBMCs) were isolated from heparinized blood of healthy donors using a Ficoll-Paque Plus density gradient (Sigma). B lymphocytes were then isolated by positive selection using anti-CD19 Microbeads (Miltenyi Biotec) and separated in a MACS LS column (Miltenyi Biotec). The purity of B lymphocytes was determined by fluorescence-activated cell sorting (FACS) assay using mouse antibodies to CD20. B lymphocytes with a purity of >95% were used for experiments. The presence of *in vivo* EBV infection of B lymphocytes was determined by qPCR assay, and only EBV-negative cells were used for infection of transcytosed EBV from the lower chambers of filter inserts.

B lymphocytes (2×10^6 cells per insert) were used for infection by transcytosed EBV from the lower chambers of filter inserts. One set of cells was infected directly with the EBV B95-8 virus that was used for transcytosis. Another set of cells was not infected and was used as a control. After 7 days, infected B lymphocytes were treated or not with 30 ng/ml of PMA to induce the lytic cycle of EBV. PMA-induced B cells were used to measure the expression of the EBV lytic genes BZLF1 and gp350/220 by quantitative reverse transcription-PCR (qRT-PCR) assay. Expression of the latent EBV LMP1 and EBNA1 genes was examined in non-PMA-induced cells. For qRT-PCR, total RNA from each sample was extracted using the RNeasy kit (Qiagen, Valencia, CA) according to the protocols provided by the manufacturer. Reverse transcription reactions were performed using the iScript reverse transcriptase kit from Bio-Rad (Hercules, CA) according to the manufacturer's protocol. The target gene was amplified from cDNA using SYBR green real-time PCR master mix (Life Technologies, Grand Island, NY), a 1 mM concentration of each primer, and 5 μl of the cDNA in a total volume of 20 μl. The following primers were used: LMP1 (forward, 5′-CAG TCA GGC AAG CCT ATG A-3′; reverse, 5′-CTG GTT CCG GTG GAG ATG A-3′), EBNA1 (forward, 5′-TAC AGG ACC TGG AAA TGG CC-3′; reverse, 5′-TCT TTG AGG TCC ACT GCC G-3′, gp350/220 (forward, 5′-AGA ATC TGG GCT GGG ACG TT-3′; reverse, 5′-ACA TGG AGC CCG GAC AAGT-3′), and BZLF1 (forward, 5′-AAA TTT AAG AGA TCC TCG TGT AAA ACA TC-3′; reverse, 5′-CGC CTC CTG TTG AAG CAG AT-3′). The beta-2-microglobulin gene was used as an internal control (forward, 5′-TGA CTT TGT CAC AGC CCA AGA TA-3′; reverse, 5′-CGG CAT CTT CAA ACC TCC A-3′) (70). EBV gene expression was calculated by the $\Delta\Delta CT$ method (71, 72).

EBV-induced cell proliferation in B lymphocytes was examined using a bromodeoxyuridine (BrdU) cell proliferation kit (Cell Signaling Technology). Freshly purified B lymphocytes were infected with transcytosed EBV B95-8, and cells were cultured for 7 days. One set of cells was not infected and served as a control. EBV-infected and uninfected cells were treated with BrdU, and BrdU incorporation into newly synthesized DNA was detected by an anti-BrdU mouse monoclonal antibody according to the manufacturer's protocol.

Electron microscopy. Cells were fixed with 2% glutaraldehyde and 4% formaldehyde in 0.1 M sodium cacodylate buffer, pH 7.3. Cells were postfixed with 1% osmium tetroxide alone or with 1.5% potassium ferricyanide followed by 2% uranyl acetate and then dehydrated with ethanol. Cells were embedded in Eponate812 or EmBed812. Ultrathin sections were stained with 2% uranyl acetate and examined at 120 kV in a JEOL 1400 transmission electron microscope.

Statistical analysis. The significance of differences between EBV apical to basolateral and basolateral to apical transcytosis through polarized epithelial cells pretreated with different drugs was determined using the Student *t* test; *P* values of <0.05 were considered significant.

RESULTS

Establishment of a polarized oral epithelial cell model for EBV bidirectional transcytosis. To study EBV bidirectional transcytosis, we established polarized primary tonsil keratinocytes. For apical to basolateral transcytosis experiments, cells were grown on the upper surfaces of Transwell filter inserts, with the apical cell surfaces facing up, and virus was added to the apical surfaces (Fig. 1A). For basolateral to apical transcytosis, cells were grown on the lower surfaces of filter inserts, with the apical cell surfaces facing the lower chamber and the basal cell surfaces attached to the lower face of the filter inserts as described previously (73) (Fig. 1B). For this, filter inserts were placed upside down in petri dishes, and cells in 50 μl of medium were added to the filter surface. Inserts with cells were incubated for 2 to 3 h at 37°C in 5% CO_2 to allow attachment of cells to the filters. Filter inserts were then placed into 12-well plates in the correct orientation. Attached keratinocytes then formed polarized monolayers with apical membranes facing the lower chamber and the basal membrane attached to the filter insert at its lower surface. Adding virus to the upper chambers of these inserts permitted binding of virions to the basal surface of polarized cells.

After plating, cells were maintained for 10 to 14 days. Cells in each insert were then measured for transepithelial resistance (TER), and one or two inserts from each plate was examined for the presence of tight junctions by confocal and/or electron microscopy. For confocal microscopy, polarized cells were immunostained for the tight junction proteins ZO-1 (Fig. 1, right images) and occludin (data not shown). Thus, cell polarity was evaluated by two criteria, and cells were considered fully polarized when (i) electron and/or confocal microscopy showed monostratified epithelium with well-developed tight junctions that formed on the upper or lower faces of filter inserts (Fig. 1, middle and right images) and (ii) TER values reached 600 to 800 Ω/cm^2. After confirmation of cell polarity in each experiment, tonsil epithelial cells were used for EBV transcytosis assays.

Transcytosis of EBV through polarized tonsil epithelial cells is bidirectional. EBV transcytosis was examined in polarized TNSL#2 tonsil epithelial cells for both the apical to basolateral and basolateral to apical directions. We used EBV B95-8, and viral

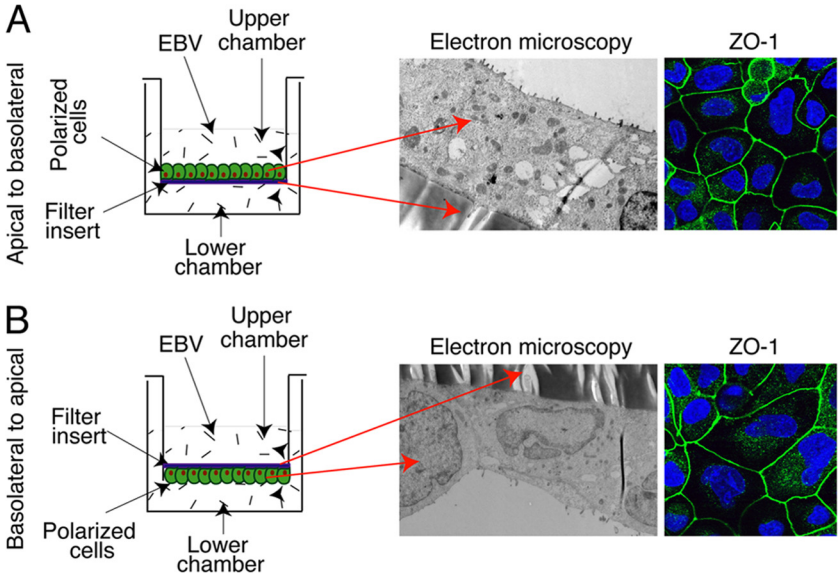

FIG 1 Model of EBV bidirectional transcytosis. (A) To study apical to basolateral transcytosis, cells were grown on the upper surfaces of Transwell filter inserts, with apical surfaces facing upward, and virus was added to the apical membranes. (B) To study basolateral to apical transcytosis, cells were grown on the lower surfaces of Transwell filter inserts, with apical membranes facing the lower chambers. Addition of virus to the upper chambers of the Transwell inserts allows binding of virions to the apical (A) or basal (B) surfaces of polarized cells. Detection of virus in the culture media of lower chambers indicates EBV transcytosis in the apical to basolateral (A) and basolateral to apical (B) directions. (Middle images) Polarized cells were examined by electron microscopy. Red arrows indicate cells and filter inserts. (Right images) Polarized cells were immunostained for the tight junction protein ZO-1 and analyzed by confocal microscopy. Nuclei are stained in blue with TO-PRO3. Original magnification, ×600.

titers were calculated based on encapsidated DNA copy number. EBV concentrations in saliva may vary between 5×10^7 and 10^8 per ml (29), indicating that EBV transmission through saliva may involve high concentrations of salivary virions. Therefore, for transcytosis assays, we used 10^7 virions per insert. Virus was added to the upper chambers of Transwell inserts with either apically or basolaterally oriented polarized epithelial cells. After 1, 2, 3, and 4 h, culture media from the lower chambers were examined for EBV by qPCR. Two hours after incubation, EBV DNA was detected in the lower chambers in the transcytosis assay for the basolateral to apical direction (Fig. 2A). At 3 h and 4 h postincubation, EBV DNA was detected in the lower chambers in transcytosis assays for both directions, indicating that EBV transcytosis may occur in both directions. However, EBV transcytosis in the apical to basolateral direction was found to be about 2-fold lower than that in the basolateral to apical direction. Detection of about 10^5 virion DNA copies in the apical to basolateral transcytosis assay and 2×10^5 DNA copies in the basolateral to apical transcytosis assay at the 4-h time point suggested that approximately 1% and 2% of total input virions traversed the polarized monolayers in the apical to basolateral and basolateral to apical directions, respectively. However, as the majority of virions could be trapped in the filters (18, 74), we examined the passage of virions through Transwell inserts in the absence of cells. EBV B95-8 virus at 10^7 DNA copies per insert was added to the upper chambers of inserts without cells, and virions collected from the basolateral chambers were quantified by qPCR. These measurements showed that about 1.1×10^6 virion DNA copies were present in the basolateral chambers, indicating that approximately 90% of virions are trapped within the filter pores. Thus, the real efficiencies of EBV transcytosis in the apical to basolateral and basolateral to apical directions are approximately 10 and 20%, respectively.

Next, we compared bidirectional EBV transcytosis in polarized tonsil epithelial cells propagated from 8 independent donors (Fig. 2B). Apical to basolateral EBV transcytosis was detected in 5 of 8 (62%) epithelial cultures obtained from independent donors. EBV basolateral to apical transcytosis was observed in 6 of 8 (75%) polarized epithelial cultures. The efficiency of viral transcytosis varied between polarized cells obtained from different individuals. Apical to basolateral transcytosis varied between 0.15% and 0.35%, and basolateral to apical transcytosis varied between 0.05% and 1.3%. Interestingly, tonsil cells obtained from one donor (TNSL#7) showed only apical to basolateral transcytosis, and that from another donor (TNSL#5) showed only basolateral to apical transcytosis. In TNSL#6 cells, EBV transcytosis was not detected in either direction. TER was 600 to 800 Ω/cm^2 in all 8 cell lines (data not shown), indicating that all cells were highly polarized and that the variability in EBV transcytosis was not due to a lack of cell polarity.

The maximum duration of our transcytosis assay was 4 h, a time period insufficient for productive viral infection and secretion of progeny virions. Nevertheless, we also examined transcytosis of UV-inactivated EBV, which should not lead to productive viral infection. UV-exposed and untreated B95-8 viruses were used for apical to basolateral and basolateral to apical transcytosis through polarized tonsil epithelial cells. qPCR data showed that the levels of transcytosis of UV-inactivated and control virions were comparable in both directions (Fig. 2C), indicating that viral transcytosis occurs in the absence of productive EBV infection.

To determine if the levels of EBV transcytosis are similar across different strains of virus, we compared the transcytosis of the B95-8 and Akata strains through polarized tonsil epithelial cells. Transcytosis of the B95-8 and Akata strains in the apical to baso-

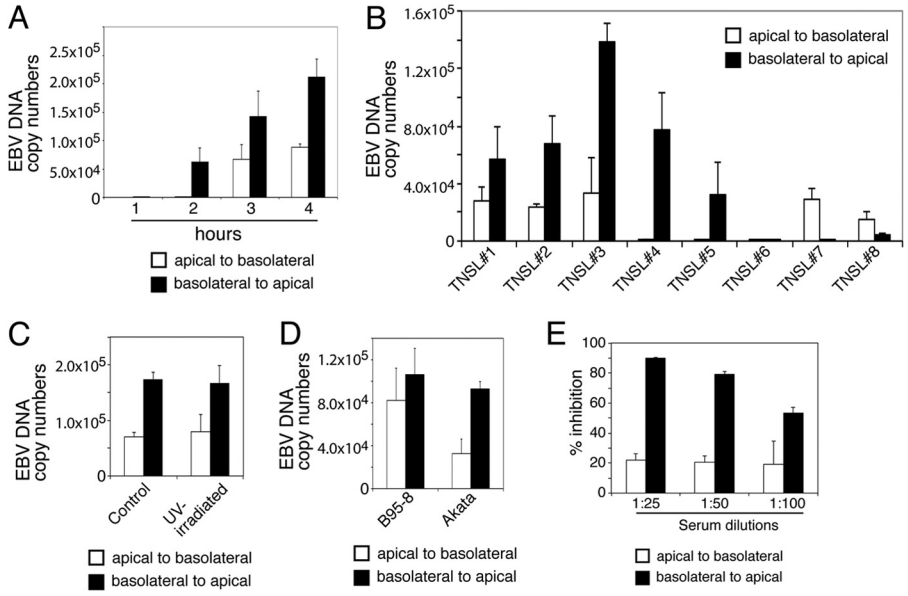

FIG 2 Bidirectional EBV transcytosis through polarized tonsil epithelial cells. (A) EBV B95-8 virus (10^7 virions) was added to the upper chambers of Transwell inserts with either apically or basolaterally oriented polarized TNSL#2 tonsil epithelial cells. After 1, 2, 3, and 4 h, culture media from the lower chambers were examined for EBV by qPCR. Similar results were obtained in 3 independent experiments. (B) Polarized cells were propagated from tonsil keratinocytes of 8 independent donors. EBV transcytosis assays were performed in the apical to basolateral and basolateral to apical directions. After 4 h, culture media from the lower chambers were examined for EBV. (C) To measure transcytosis of UV-inactivated EBV, UV-exposed and untreated B95-8 virus was used for bidirectional transcytosis assays using TNSL#2 cells. (D) EBV transcytosis via polarized TNSL#2 tonsil epithelial cells was performed using B95-8 and Akata strains of virus in the apical to basolateral and basolateral to apical directions. (E) EBV virions were incubated with pools of either EBV-positive or -negative sera from healthy individuals. These virions were then used for apical to basolateral or basolateral to apical transcytosis in TNSL#3 cells. Transcytosed virions were quantified by qPCR after 4 h. Data are presented as percent inhibition of transcytosis of virions preincubated with EBV-positive sera relative to transcytosis of virions preincubated with EBV-negative control sera. The results were similar in 2 independent experiments. Error bars show standard errors of the means.

lateral and basolateral to apical directions showed that both viral strains undergo bidirectional transcytosis through tonsil epithelial cells (Fig. 2D).

To confirm that EBV transcytosis is specific for the virus, B95-8 virions were preincubated with a pool of EBV-neutralizing human sera collected from 4 healthy EBV-seropositive individuals (66). As a control, virions were preincubated with a pool of 2 EBV-negative human sera. These virions were then used for apical to basolateral or basolateral to apical transcytosis. Analysis of transcytosed virions by qPCR showed that EBV-specific sera substantially inhibited (50 to 90%) basolateral to apical transcytosis in a dose-dependent manner. EBV sera also inhibited EBV apical to basolateral transcytosis; however, this inhibition was much weaker (~20%) than inhibition of basolateral to apical viral transcytosis (Fig. 2E).

Transcytosed EBV is infectious. To examine the infectious activity of transcytosed EBV, transcytosis assays were performed in polarized tonsil keratinocytes using B95-8 virus. After apical to basolateral and basolateral to apical transcytosis, culture media containing transcytosed virus were collected and used for infection of EBV-negative B lymphocytes. One set of B cells was directly infected with the same virus as was used for transcytosis of epithelial cells. For direct infection of B cells, a 2×10^5-DNA copy equivalent of virions was used, which is approximately the number of virions that transcytosed through polarized epithelial cells in our assays. After 7 days, B cells were treated with PMA for 3 days to induce the EBV lytic cycle. Total RNA was isolated and examined for the presence of transcripts of the lytic BZLF1 and gp350/220 genes. qRT-PCR assay detected EBV lytic gene expression in B lymphocytes infected with virions transcytosed in both the apical to basolateral and basolateral to apical directions (Fig. 3A). The infectivity of virions transcytosed in the apical to basolateral direction was approximately 0.7- to 2-fold lower than that of virions transcytosed in the basolateral to apical direction. This reflects the lower level of EBV apical to basolateral transcytosis relative to basolateral to apical transcytosis. B cells directly infected with EBV also showed expression of viral lytic genes, confirming that the virus used for transcytosis was infectious.

In the next set of experiments, we examined infection of B lymphocytes by transcytosed EBV by detecting expression of the viral latent LMP1 and EBNA1 genes and by measuring EBV-induced B cell proliferation. B lymphocytes were infected with B95-8 virus transcytosed in either the apical to basolateral or the basolateral to apical direction. Uninfected B lymphocytes served as controls. After 7 days, half of the culture was used for detection of LMP1 and EBNA1 transcripts, and the other half was used for cell proliferation assays using a BrdU kit. Analysis of LMP1 and EBNA1 expression by qRT-PCR showed that both genes were expressed in B lymphocytes infected with EBV B95-8 virus transcytosed through polarized tonsil epithelial cells (Fig. 3B). LMP1 and EBNA1 expression was not detected in uninfected B lymphocytes. Proliferation of EBV-infected B lymphocytes was 2.3-fold higher than proliferation of uninfected B cells (Fig. 3C). Thus, these experiments showed that EBV transcytosed through polarized tonsil epithelial cells infects B lymphocytes and induces their proliferation.

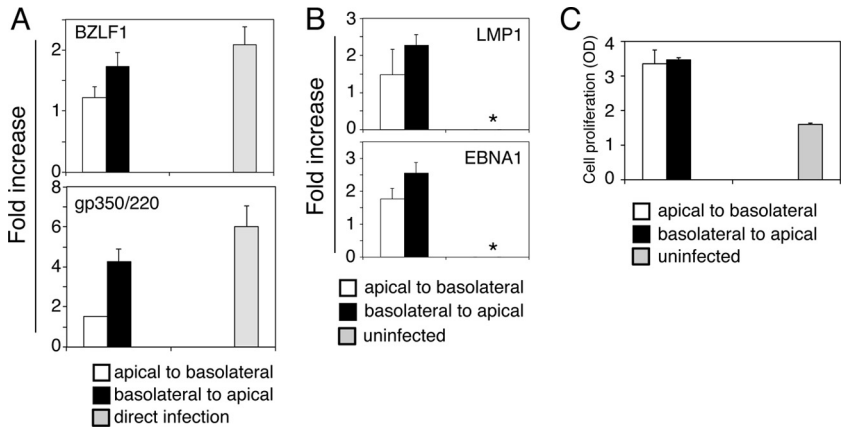

FIG 3 Infectivity of transcytosed EBV in B lymphocytes. (A) EBV B95-8 bidirectional transcytosis assays were performed in polarized TNSL#3 tonsil epithelial cells. Transcytosed virions were collected and used for infection of EBV-negative B lymphocytes. One set of cells were infected with virus that was used for transcytosis of epithelial cells (direct infection). After 7 days, B cells were treated with PMA for the next 3 days. Cells were collected, and total RNA was isolated and used for qRT-PCR assays of BZLF1 (upper graph) and gp350/220 (lower graph) gene expression. (B and C) Freshly isolated EBV-negative B lymphocytes were infected with EBV B95-8 virions transcytosed through polarized TNSL#3 tonsil epithelial cells. One set of B lymphocytes was not infected and served as a control. (B) After 7 days, half of the cultures were used for qRT-PCR assays of LMP1 and EBNA1 gene expression. *, not detected. (C) The other half of the B lymphocyte cultures were used for cell proliferation assays. OD, optical density. Error bars show standard errors of the means. Similar results were obtained in 2 independent experiments.

Apical to basolateral transcytosis of EBV is initiated by macropinocytosis, whereas basolateral to apical transcytosis of EBV is initiated by caveolin-mediated endocytosis. To study the mechanisms of EBV transcytosis, polarized tonsil epithelial cells were pretreated with nontoxic concentrations of chlorpromazine (20 μM) or nystatin (12.5 μg/ml), which are inhibitors of clathrin- and caveolin-mediated endocytosis, respectively (75–78). In parallel experiments, cells were treated with nontoxic concentrations of amiloride (100 μM) (79), which inhibits macropinocytosis. Untreated cells served as a control. After treatment, cells were washed and used for apical to basolateral or basolateral to apical transcytosis assays.

After 1 h of drug treatment and 4 h of viral exposure, the TER of polarized cells was measured (Fig. 4A). The TER data showed that chlorpromazine and amiloride did not reduce TER; however, nystatin reduced it by about 15%. EBV was added to the upper chambers of apically or basolaterally oriented polarized cells, and after 4 h of incubation, culture media from the lower chambers were collected for qPCR assay. After transcytosis assays, polarized cells were examined for paracellular permeability to validate polarized monolayer integrity (Fig. 4B). No leakage was detected in any of the drug-treated cells, including those treated with nystatin, indicating the presence of intact tight junctions. One set of cells was also used for viability assays, which showed that drug-treated and control cells had similar values (Fig. 4C). Altogether, the data indicated that drug treatment and viral inoculation had no toxic effect on the polarized cells.

Culture media collected from the lower chambers were used for detection of EBV by qPCR. Quantitation of transcytosed virions showed that pretreatment of polarized cells with the inhibitor of caveolin-mediated endocytosis nystatin reduced EBV transcytosis in the basolateral to apical direction (about 70%) (Fig. 4D), indicating that caveolin-mediated endocytosis plays a critical role in EBV basolateral to apical transcytosis. In contrast, chlorpromazine did not reduce EBV transcytosis in either direction; i.e., clathrin-mediated endocytosis did not play a significant role in EBV transcytosis. Amiloride substantially reduced (about 80%) apical to basolateral but not basolateral to apical EBV transcytosis, indicating a critical role for macropinocytosis in apical to basolateral transport of virus. To confirm amiloride-mediated inhibition of EBV apical to basolateral transcytosis, polarized cells were treated with increasing concentrations of amiloride (Fig. 4E). Measurement of viral transcytosis across these cells showed that amiloride-mediated inhibition of EBV apical to basolateral transcytosis was dose dependent. Similarly, we confirmed nystatin-mediated inhibition of basolateral to apical transcytosis by treating cells with increasing concentrations of nystatin (Fig. 4F). Basolateral to apical transcytosis assays in these cells showed that nystatin-mediated inhibition of EBV basolateral to apical transcytosis was also dose dependent. Amiloride and nystatin also inhibited apical to basolateral and basolateral to apical transcytosis, respectively, of the EBV Akata strain (data not shown).

To determine whether drug treatment changed virus binding to cell surfaces, polarized cells were pretreated with nystatin, chlorpromazine, or amiloride for 1 h and then washed and incubated with EBV B95-8 virus at the apical or basolateral membrane. As shown in our model (Fig. 1), virus binding to apical membranes does not require crossing of virions through the Transwell filters. In contrast, in order to reach the basolateral membranes, the virus needs to overcome the filter barrier, which blocks approximately 90% of virions from passing through filter pores. To solve this problem and to establish equal numbers of virions for apical and basolateral binding, we added a 10-fold excess of viral inoculum for basolateral binding. Thus, 10^6 and 10^7 virions were added to the upper chambers of inserts with apically and basolaterally oriented polarized cells, respectively. Cells were incubated at 4°C for 2 h for virus binding. The qPCR results revealed that EBV binding to basolateral membranes was about 2-fold higher than binding to apical membranes. Trypsin treatment of cells stripped surface-bound virions from both apical and basolateral membranes, confirming virus binding to cell membranes. Higher basolateral binding was consistent with the higher rate of basolateral

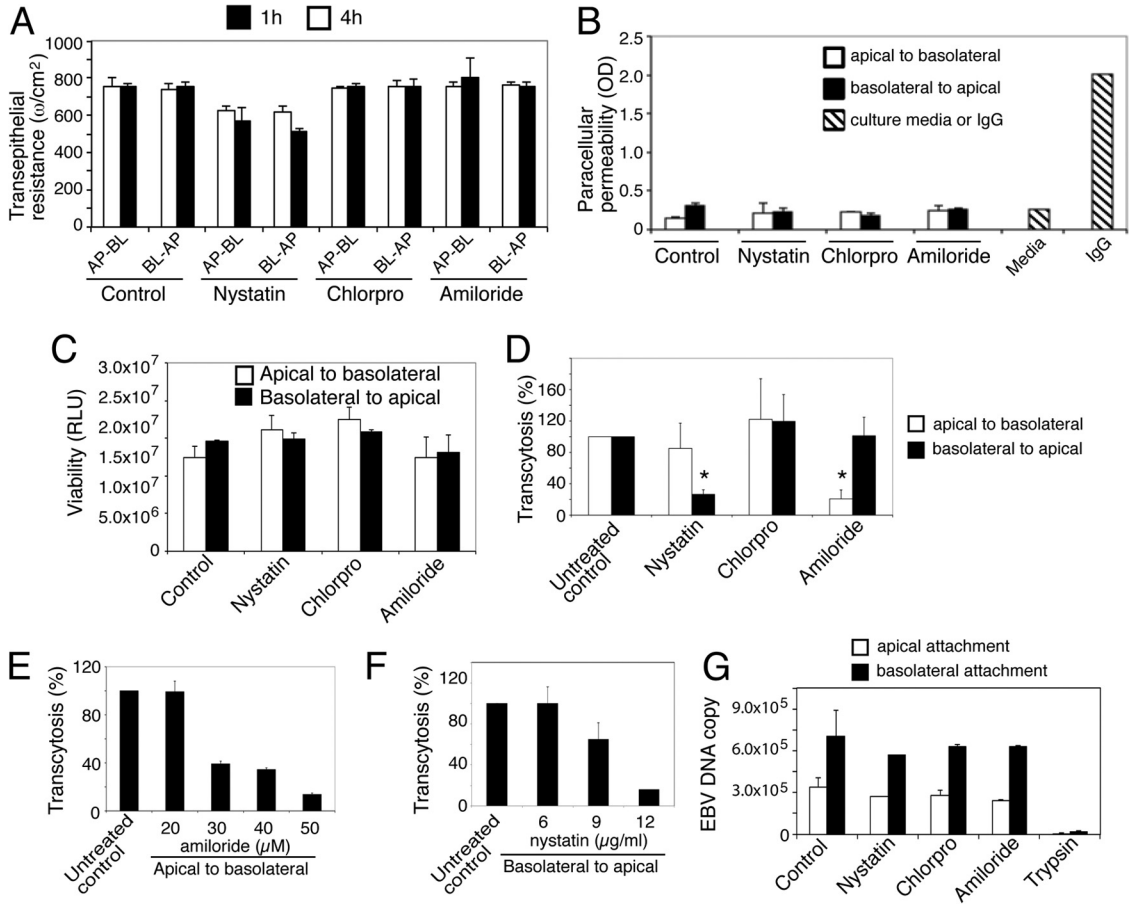

FIG 4 EBV apical to basolateral transcytosis is facilitated by macropinocytosis, whereas basolateral to apical transcytosis is initiated by caveolin-mediated endocytosis. (A) Polarized TNSL#3 tonsil epithelial cells were pretreated with nystatin, chlorpromazine, or amiloride for 1 h. Cells were washed and TER was measured. These cells were then used for EBV B95-8 bidirectional transcytosis and after 4 h, TER was again measured. (B) After transcytosis assays, cells were subjected to paracellular permeability assays. Media, culture media without IgG that served as negative control; IgG, horseradish peroxidase-labeled IgG that was added to the upper chamber. (C) One set of cells after transcytosis was used for cell viability assays. (D) Drug-pretreated polarized cells were used for bidirectional transcytosis assays with 10^7 virions per insert. Transcytosed EBV from the lower chamber of control and drug-treated cells was quantitated by DNA qPCR. Data are presented as percent viral transcytosis in drug-treated cells relative to untreated controls. Controls were considered 100%. Average percent transcytosis is presented from 5 independent experiments. *, $P < 0.001$ compared with the untreated control cells. (E) Polarized TNSL#3 cells were treated with increasing concentrations of amiloride, and apical to basolateral EBV transcytosis was examined by qPCR assay. (F) TNSL#3 cells were treated with increasing concentrations of nystatin, and basolateral to apical transcytosis of EBV was examined. (G) Polarized TNSL#3 cells were pretreated with nystatin, chlorpromazine, or amiloride at 37°C for 1 h. Cells were then washed and exposed to EBV B95-8 from their apical and basolateral membranes at 4°C for 2 h. One set of control cells was trypsinized to remove membrane-bound virions. Cells were washed and lysed, and viral binding was examined by qPCR. Results are presented as copy numbers of viral DNA in control and drug-treated cells. Results shown are from one representative experiment out of two experiments. Chlorpro, chlorpromazine; RLU, relative luminescence units. Error bars show standard errors of the means.

to apical transcytosis. None of the drug pretreatments significantly affected viral binding, demonstrating their role specifically in virus entry (Fig. 4G).

Characterization of EBV macropinocytosis by electron microscopy. To visualize macropinocytosis of EBV, polarized tonsil epithelial cells were exposed to EBV at their apical membranes for 30 min and then analyzed by electron microscopy. Apically incubated virions were surrounded by membrane protrusions (Fig. 5A, green arrowheads, inset) and membrane invaginations (Fig. 5B, green arrowheads, inset). Virions were also detected in subapical uncoated endocytic vesicles (Fig. 5B and C, blue arrowheads, inset) of approximately 0.2 to 2.5 μm diameter, typical sizes for macropinosomes (80–82). Similar electron microscopy data have been obtained for macropinocytosis of other viruses, including Kaposi's sarcoma-associated herpesvirus (KSHV), human cytomegalovirus (HCMV), human immunodeficiency virus (HIV), African swine fever virus, and influenza virus (83–87). Thus, these ultrastructural features of EBV apical entry are characteristics of EBV macropinocytosis. Association of EBV with clathrin-coated pits of vesicles was not observed.

Effect of macropinocytosis and dynamin inhibitors on EBV transcytosis. Macropinocytosis is a multistep process, and membrane ruffling and protrusion formation are among the initial steps which lead to the generation of macropinosomes containing viral particles (88–95). These critical events require induction of complex signaling pathways involving activation of phosphatidylinositol 3-kinases (PI3K), protein kinase C (PKC), and myosin light-chain kinase (MLCK). To better characterize the molecular mechanism of EBV macropinocytosis, polarized cells were pretreated with nontoxic concentrations of the following inhibi-

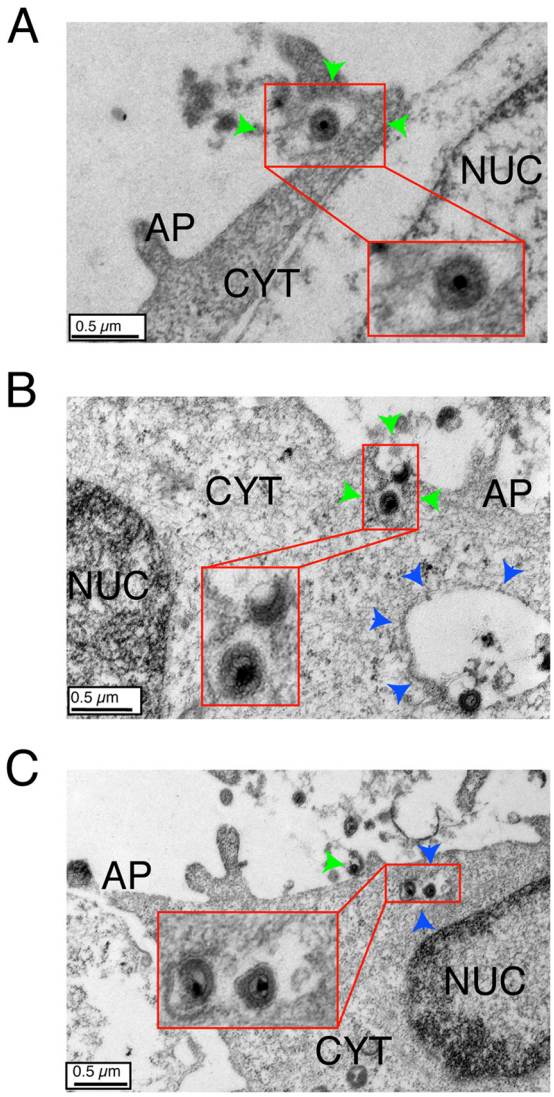

FIG 5 Visualization of EBV macropinocytosis from apical membranes of polarized tonsil epithelial cells. Polarized TNSL#3 tonsil epithelial cells exposed to EBV B95-8 at their apical membranes were fixed after 30 min and analyzed by electron microscopy. (A) EBV virions surrounded by apical membrane protrusions. (B) Virions are in the invaginated membranes and subapical macropinosome-like vesicles. (C) Virions in the subapical macropinosomes. Insets and green arrowheads show membrane-bound and penetrating virions. Blue arrowheads show virions in the macropinosomes. AP, apical; CYT, cytoplasm; NUC, nuclei.

tors: LY294002 (100 μM) for PI3K, rottlerin (100 μM) for PKC, and ML9 (5 μM) for MLCK. Since dynamin may be involved in macropinocytosis, cells were also treated with the dynamin inhibitor dynasore (100 μM). Polarized cells were treated with inhibitors for 1 h and then washed and measured for TER. None of the drug treatments caused a reduction in TER (data not shown). Cells were then used for EBV apical to basolateral and basolateral to apical transcytosis assays. qPCR data showed that inhibitors of PI3K and dynamin reduced EBV transcytosis in both directions (Fig. 6A). However, inhibition of PI3K reduced EBV transcytosis mainly in the apical to basolateral direction, in contrast to dynamin inhibition, which predominantly reduced viral transcytosis in the basolateral to apical direction. Inhibitors of PKC and MLCK reduced EBV apical to basolateral transcytosis (Fig. 6A), but their effects on basolateral to apical transcytosis were not significant.

Macropinocytosis also requires the activation of Ras-related C3 botulinum toxin substrate 1 (Rac-1), p21-activated kinase-1 (Pak1), ADP-ribosylation factor 6 (ARF6), and cell division control protein 42 homolog (Cdc42). To determine the role of these molecules in EBV transcytosis, polarized tonsil cells were transfected with siRNAs against Rac-1, Pak1, Cdc42, and ARF6. We also used siRNA against dynamin. After 48 h, one set of cells was used for Western blot analysis, which showed silencing of expression of Rac-1, Pak1, Cdc42, ARF6, and dynamin (Fig. 6B). The next set of cells was used for EBV transcytosis. qPCR analysis of EBV transcytosis showed that silencing of Rac-1, Cdc42, and dynamin reduced both apical to basolateral and basolateral to apical virion transcytosis. Silencing of Pak1 and ARF6 reduced apical to basolateral transcytosis but did not affect basolateral to apical transcytosis (Fig. 6C).

Although it is well known that actin polymerization plays a critical role in macropinocytosis (94), we were unable to test the role of actin polymerization in EBV transcytosis, as blocking of actin polymerization with cytochalasin B in polarized cells caused rapid depolarization of epithelial cells (data not shown).

Caveolin-mediated endocytosis plays a role in EBV basolateral to apical transcytosis. Above (Fig. 4D), we showed that pretreatment of polarized cells with a pharmacological inhibitor of caveolin-mediated endocytosis reduced mainly basolateral to apical viral transcytosis and that an inhibitor of clathrin-mediated endocytosis did not reduce EBV transcytosis in either direction. To confirm these findings, we coimmunostained polarized cells fixed 30 min after the start of transcytosis for EBV p18 and clathrin or caveolin-1, which are markers of clathrin- or caveolin-containing endocytic vesicles, respectively (Fig. 7). Confocal microscopy showed that EBV p18 colocalization with clathrin was not detected in either direction (Fig. 7A and B, upper images), indicating that clathrin-mediated endocytosis does not play a role in EBV entry from both membranes of polarized cells. In contrast, EBV p18 strongly colocalized with caveolin in the basolateral to apical transcytosis assay (Fig. 7B, lower images) but not in the apical to basolateral assay (Fig. 7A, lower images). These data indicate that virion entry from basolateral membranes is initiated by caveolin-mediated endocytosis leading to basolateral to apical transcytosis of virus.

We then examined the role of caveolin- and clathrin-mediated endocytosis in EBV transcytosis by inactivating caveolin-1 and clathrin heavy-chain expression using an siRNA approach. Polarized cells were transfected with specific siRNAs against the caveolin-1 and clathrin heavy-chain genes or with control siRNAs. Forty-eight hours later, one set of cells was subjected to Western blot analysis for detection of caveolin-1 and clathrin heavy-chain expression. The data showed that specific siRNA transfection led to about 50% and 70% reductions in expression of clathrin heavy-chain and caveolin-1, respectively (Fig. 8A). In a second set of cells, EBV transcytosis assays were performed. qPCR data revealed that silencing of the caveolin-1 gene reduced basolateral to apical transcytosis but not apical to basolateral transcytosis (Fig. 8B). Inactivation of clathrin heavy chain did not cause a significant reduction in EBV transcytosis in either direction.

Caveolae and caveosomes are localized to basolateral membranes, and their depletion inhibits EBV basolateral to apical transcytosis. It has been shown that localization of caveolae and

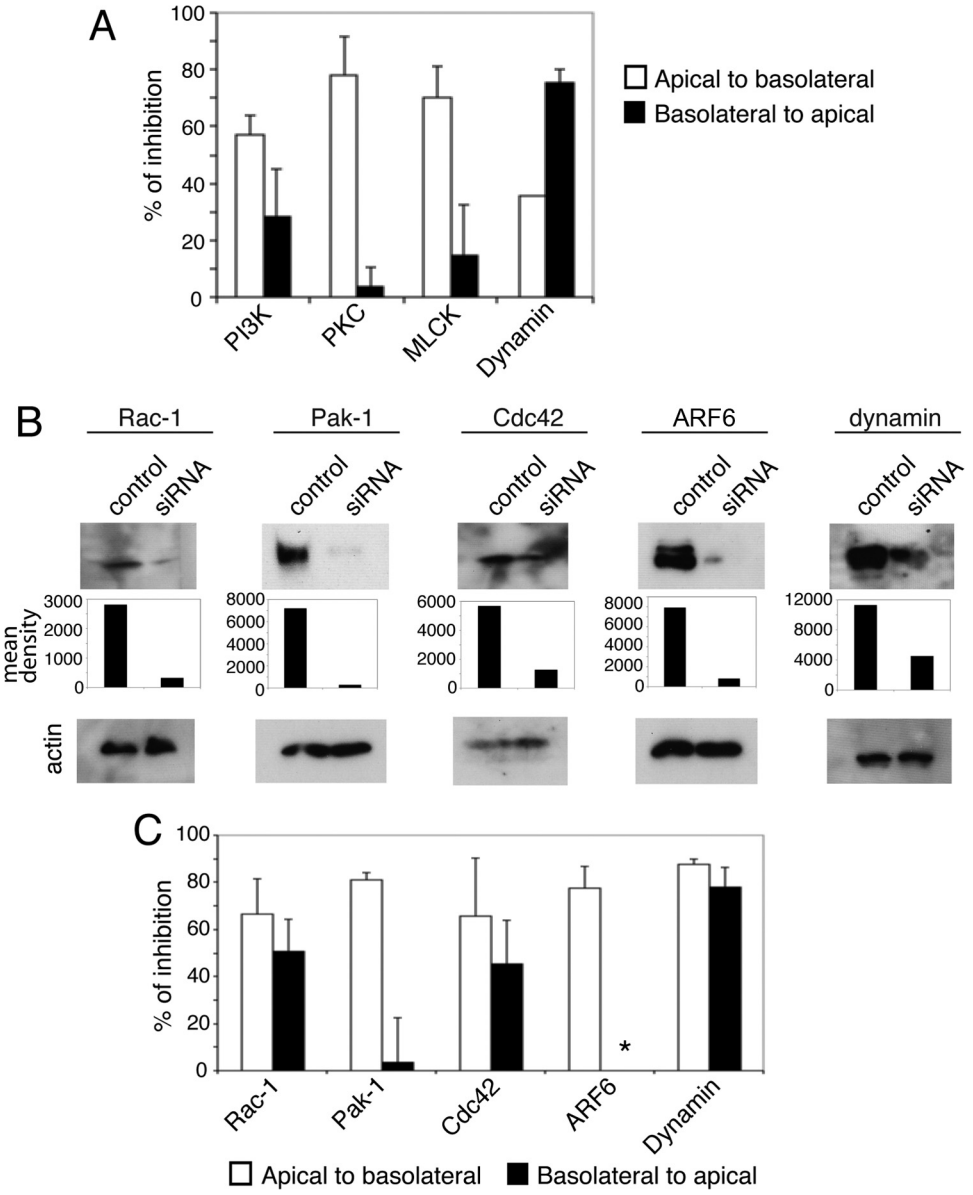

FIG 6 Inhibition of EBV transcytosis by drugs and siRNAs. (A) Polarized TNSL#3 tonsil epithelial cells were pretreated with inhibitors of PI3K (LY294002), PKC (rottlerin), MLCK (ML9), and dynamin (dynasore) for 1 h. Cells were then washed and used for EBV B95-8 bidirectional transcytosis assays. After 4 h, viral transcytosis was examined using qPCR. Data are presented as percent inhibition of EBV transcytosis by drug treatment relative to untreated controls. Average percent inhibition is presented from 2 independent experiments. (B) Polarized tonsil cells transfected with specific siRNAs against Rac-1, Pak1, Cdc42, ARF6, or dynamin 1/2. An irrelevant siRNA was used as a control. After 48 h, one set of cells was used for Western blot analysis using antibodies against Rac-1, Pak1, Cdc42, ARF6, or dynamin 2. The mean densities of pixels in the protein bands were measured by ImageJ software, and the results for each gel are shown as a bar graph under each blot. (C) The next set of cells was used for EBV transcytosis, which was evaluated by qPCR assay. Data are presented as percent inhibition of viral transcytosis by drugs relative to untreated controls. Average percent inhibition is presented from 2 independent experiments. *, no inhibition was detected. (A and C) Error bars show standard errors of the means.

caveosomes in polarized kidney and intestinal epithelial cells is predominantly restricted to basal and lateral membranes (96). Distribution of caveolin-1 in polarized membranes was also found to be predominantly basolateral (97) and not to play a major role in the apical membrane transport machinery (98). To determine if EBV basolateral entry occurs via caveolin and caveosomes, EBV was added to basolateral membranes of polarized cells, and after 30 min, cells were fixed and analyzed by transmission electron microscopy. We detected the presence of multiple virions within the intercellular space of lateral membranes (Fig. 9A). Many virions were attached to the lateral membranes with uncoated invaginations (Fig. 9A, inset and arrowheads; Fig. 9B, inset). The morphology of these invaginations was similar to that of basolaterally localized caveolae (96). Moreover, EBV was detected in cytoplasmic endosomes (Fig. 9C, inset), which might be caveosomes that were generated by virus-bound caveolae. Localization of virions to clathrin-coated pits and vesicles was not detected.

Association of caveolin-1 with cholesterol (99) is critical for

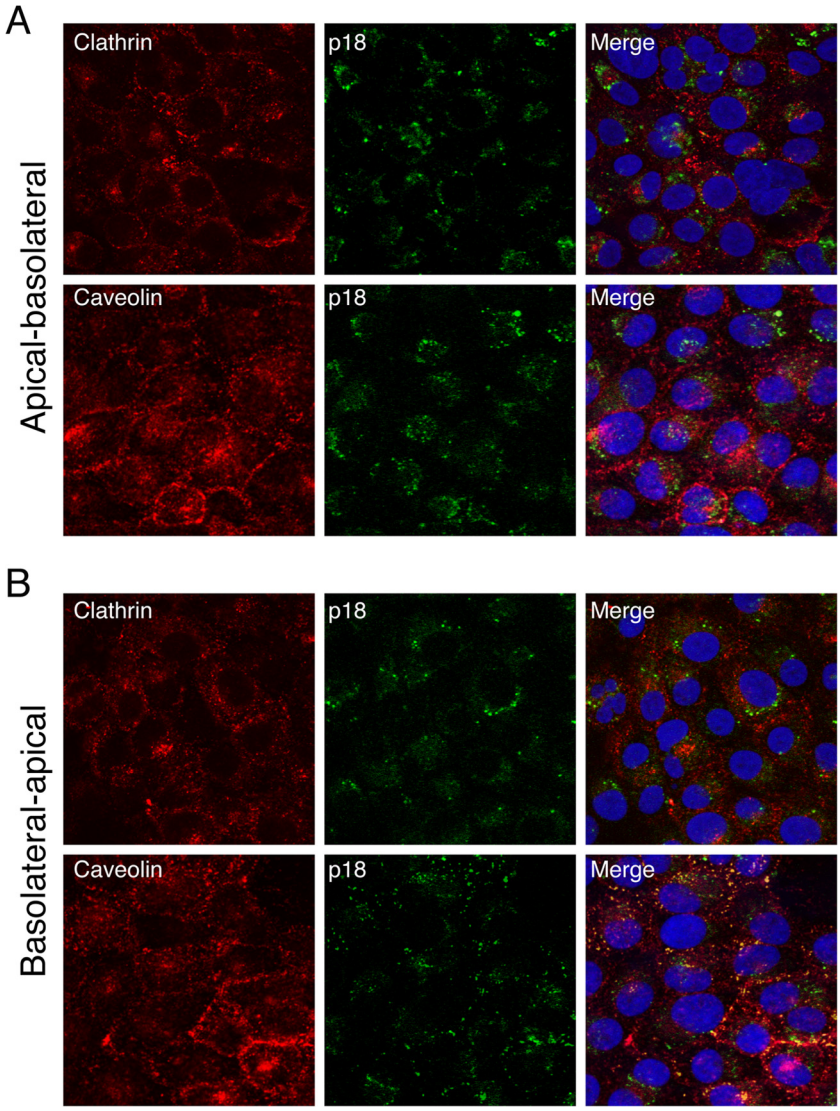

FIG 7 EBV p18 colocalizes with caveolin-containing vesicles upon entry of virus from basolateral membranes of polarized cells. Polarized TNSL#3 tonsil epithelial cells were exposed to EBV B95-8 from apical (A) or basolateral (B) membranes, and 30 min later, cells were fixed and coimmunostained for EBV p18 (green) and either clathrin (red) or caveolin-1 (red). Cells were analyzed by confocal microscopy. Yellow in panel B (lower right image) indicates colocalization of EBV p18 with caveolin-associated vesicles. Nuclei are stained in blue. Original magnification, ×600.

caveolin-mediated endocytosis (100). To determine the role of caveolin-mediated endocytosis in EBV transcytosis, polarized oral epithelial cells were subjected to domain-specific depletion of cholesterol. It has been shown that application of methyl β-cyclodextrin (MβCD) to the apical or basolateral membranes of polarized epithelial cells results in the release of cholesterol specifically from the treated membranes (67). MβCD does not penetrate cells but rather interacts with the cell surface and causes release of membrane cholesterol into the medium (67). Cells were treated with 10 mM MβCD at the apical and/or basolateral membranes for 15 min. Analysis of apical and basolateral media showed that MβCD treatment resulted in the release of cholesterol specifically from the treated membrane and not from the untreated membrane (Fig. 10A). The TER of MβCD-treated polarized cells was stable for 2 h after treatment (Fig. 10B), but after 2 h, it was substantially reduced (data not shown); i.e., the tight junctions of these cells were disrupted. Therefore, we were not able to perform transcytosis assays, which require 4 h of incubation of virus with the intact polarized cells. Due to this restriction, instead of examining transcytosis directly, we examined EBV entry, which does not require longer incubation times. After MβCD treatment, cells were washed with cold PBS and incubated with EBV at the apical or basolateral membranes for 1 h at 37°C. After 1 h of viral incubation, cells were collected by trypsinization (using 0.25% trypsin), and EBV entry was then measured by qPCR. Depletion of cholesterol from apical membranes did not significantly reduce EBV entry (Fig. 10C). In contrast, cholesterol depletion from basolateral membranes reduced EBV entry by about 90%, indicating that caveolin-mediated viral endocytosis may play a critical role in EBV basolateral to apical transcytosis.

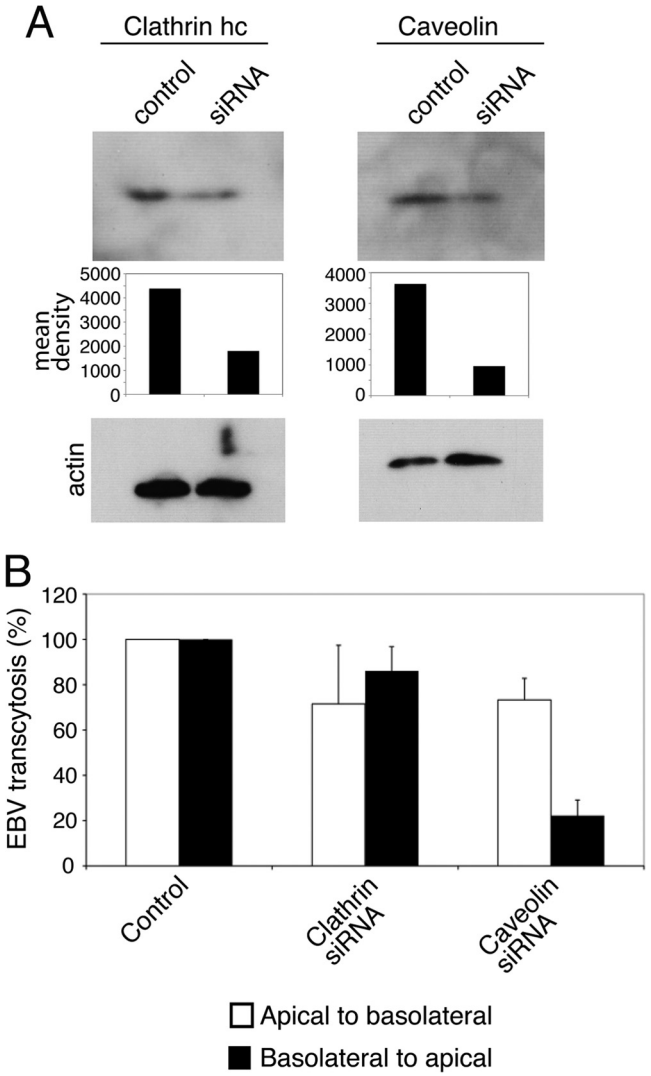

FIG 8 EBV basal to apical transcytosis initiated by caveolin-mediated endocytosis. (A) Polarized TNSL#3 cells transfected with specific siRNAs against clathrin heavy chain or caveolin-1. After 48 h, one set of cells was used for detection of clathrin heavy chain or caveolin-1 on Western blots. The mean densities of pixels in the protein bands are shown as a bar graph under each blot. (B) The next set of siRNA-transfected cells was used for EBV B95-8 transcytosis. Viral transcytosis was evaluated by qPCR, and data are presented as percent EBV transcytosis in specific siRNA-transfected cells relative to cells transfected with control siRNAs. Viral transcytosis in controls was considered to be 100%. Average percent transcytosis is presented from 2 independent experiments. Error bars show standard errors of the means.

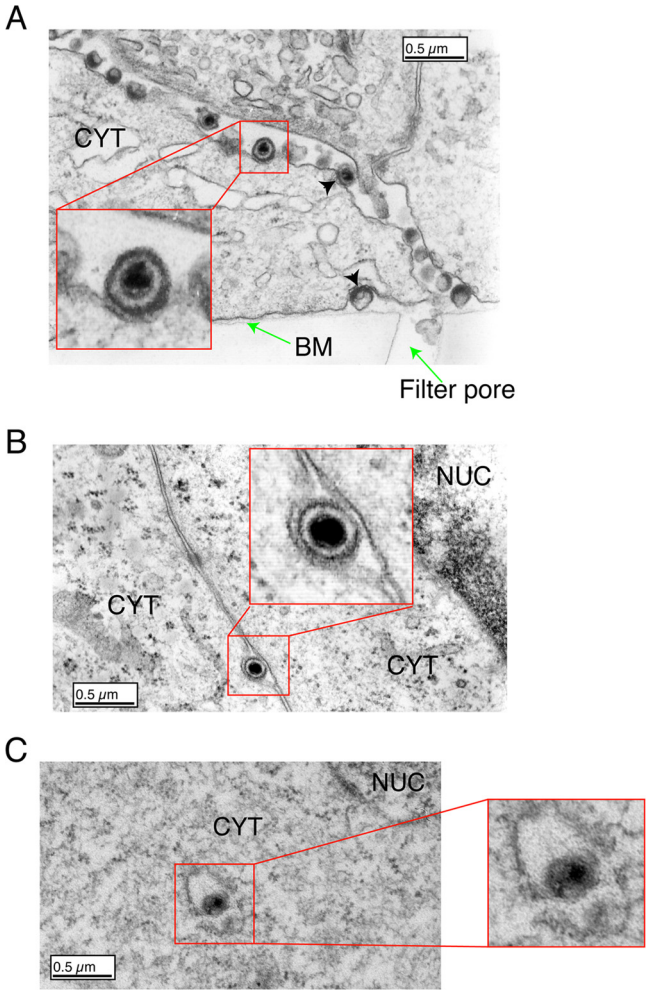

FIG 9 Detection of caveolae and EBV-containing caveosomes in basolateral membranes of oral epithelial cells. Polarized TNSL#3 tonsil epithelial cells were exposed to EBV B95-8 from their basolateral membranes, and after 30 min, cells were fixed and analyzed by electron microcopy. (A, inset and arrowheads) Multiple EBV virions were detected within the basolateral membranes of polarized cells, and virions were bound to invaginated membranes. (B, inset) Virions were detected in the deeply invaginated membranes. (C, inset). EBV was detected in the endosome. BM, basal membranes; CYT, cytoplasm; NUC, nuclei.

DISCUSSION

The current working model of primary EBV entry into the human body suggests that first virus infects oral epithelial cells, and then productive replication of virus in epithelium initiates infection of B lymphocytes, leading to systemic infection (1). However, we reported previously that the apical (mucosal) surface of the intact oral epithelium is resistant to cell-free virus infection (18, 50), suggesting the existence of an alternative mechanism for EBV transmission across the oral epithelium. Here we report that initial EBV entry into mucosal epithelium might occur by rapid viral transcytosis from apical to basolateral membranes.

EBV transcytosis across oral epithelial cells was found to be a rapid process; i.e., virions crossed polarized tonsil epithelial cells from the apical (mucosal surface) to the basolateral membranes or from basolateral membranes to apical surfaces by transcytosis within 3 to 4 h. This indicates that EBV transcytosis is independent of productive viral infection, a finding that is confirmed by transcytosis of UV-inactivated virus. EBV bidirectional transmigration occurred in keratinocytes obtained from most of the independent donors. The efficiency of transcytosis varied among donors, and some of the cultures supported only unidirectional transcytosis or no transcytosis. This could be due to a lack of viral receptors or determinants for virion binding or entry in the apical or basolateral membranes of polarized cells, which needs to be studied further.

EBV virions transcytosed in both the apical to basolateral and basolateral to apical directions were infectious in EBV-negative

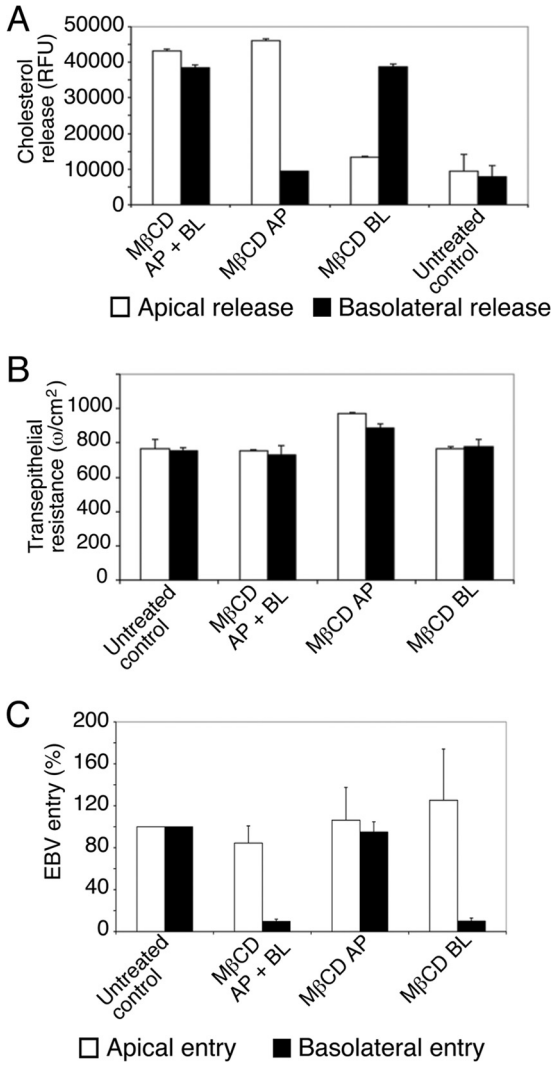

FIG 10 Cholesterol depletion inhibited EBV basolateral to apical transcytosis. (A) Polarized TNSL#1 tonsil epithelial cells were treated with methyl β-cyclodextrin from their apical and/or basolateral membranes, and culture media were collected from apical or basolateral membranes, separately. Released cholesterol was measured using the Amplex red cholesterol assay kit, and results are expressed as relative fluorescence units. (B) TER of polarized cells was measured 2 h after MβCD treatment. (C) EBV B95-8 was added to the upper chambers of apically or basolaterally oriented cells and incubated for 1 h at 37°C. Cells were then collected by trypsinization, and intracellular EBV was measured by qPCR. Data are presented as percent EBV entry into MβCD-treated cells relative to untreated controls, which was considered to be 100%. Data shown are from one representative experiment out of two experiments. Error bars show standard errors of the means.

$CD19^+$ B lymphocytes. Furthermore, transcytosed EBV induced proliferation of $CD19^+$ B lymphocytes, indicating that EBV transcytosis through the oral mucosal epithelium may play a critical role in EBV biology and pathogenesis.

Several lines of evidence presented in this paper support a key role for macropinocytosis in EBV entry from the apical membranes of oral epithelial cells, leading to apical to basolateral transcytosis of virus. We found that pretreatment of polarized oral epithelial cells with amiloride, an inhibitor of macropinocytosis, substantially reduced EBV transcytosis in the apical to basolateral direction. Macropinocytosis is an endocytic pathway that mediates the nonselective uptake of soluble molecules, nutrients, and antigens. Accumulating evidence indicates that macropinocytosis may also play a critical role in the uptake of viruses, including vaccinia virus, HIV, HCMV, herpes simplex virus (HSV), KSHV, adenovirus, ebolavirus, coxsackievirus, and paramyxovirus (41, 60, 85, 93–95, 101–110).

Macropinocytosis is initiated by activation of multibranch signaling proteins, which include the GTPases Rac-1, Cdc42, and ARF6 and the protein kinases PI3K, Pak1, PKC, and MLCK (88–95). Activation of these molecules modulates actin dynamics, leading to plasma membrane ruffling. These ruffles can be in the form of planar or circular extensions or protrusions or large extrusions (blebs). Indeed, our electron microscopy data showed EBV surrounded by protrusions at the apical surfaces of oral epithelial cells, suggesting that binding of virions to the cell surface may activate signaling molecules, leading to formation of such protrusions or ruffling. Furthermore, EBV was detected in membrane invaginations and subapical vesicles, which could be generated by folding back of membrane protrusions, forming cave-like invaginations and macropinosomes. Similar ultrastructural features have been observed in the macropinocytosis of KSHV, HCMV, HIV, African swine fever virus, and influenza virus (83–87). Inhibition of the key players in macropinocytosis—PI3K, PKC, MLCK, Rac-1, Pak1, Cdc42, and ARF6—with pharmacological agents and/or siRNAs substantially reduced EBV apical to basolateral transcytosis, confirming the role of macropinocytosis in initial EBV apical entry.

Apical to basolateral transcytosis of EBV across polarized cells indicates that separation of virion-containing macropinosomes from apical membranes initiates further delivery of virus to the intracellular endosomal compartments, leading to transcellular migration of EBV toward basolateral membranes. It has been shown that PI3K, PKC, MLCK, Rac-1, Pak1, and dynamin play roles in the closure of macropinosomes and their intracellular trafficking (88–95). Reduction in EBV transcytosis through inhibition of these signaling molecules confirmed their roles in the formation of macropinosomes and EBV transcellular migration. We further demonstrated a role for macropinocytosis in virus entry from the apical membrane by inhibiting dynamin. Dynamin may play a direct or indirect role in multiple aspects of macropinocytosis, including modulation of Rac-1 localization, actomyosin contractile activity, closure of circular ruffles, and trafficking of macropinosomes (111, 112). We found that inhibition of dynamin by dynasore pretreatment and siRNA reduced EBV apical and basolateral transcytosis.

Inhibition of clathrin-mediated endocytosis did not significantly inhibit EBV transcytosis in either direction, consistent with the absence of EBV from clathrin-coated vesicles.

We found that EBV interaction with the basolateral membranes of polarized oral epithelial cells leads to transcytosis of virions to apical membranes, and this pathway of virus transmigration depended on caveolin-mediated viral entry. Inactivation of caveolin by nystatin-mediated sequestration of cholesterol and silencing of caveolin expression with siRNA substantially reduced EBV basolateral to apical transcytosis. Electron microscopy showed the presence of caveolae in the basolateral membranes, and EBV was detected in caveosome-like endosomes. Finally, depletion of basolateral cholesterol, which prevents caveola formation, substantially inhibited EBV entry. Thus, data obtained by

three independent approaches were consistent with caveolin-mediated EBV entry at basolateral membranes of oral epithelial cells. A critical role for caveolin and cholesterol in the basolateral to apical transcytosis of polymeric IgA receptor and scavenger receptor BI has been reported (113, 114).

Dynamin is also a critical player in caveolin-mediated endocytosis (115, 116). Our data showed that inactivation of dynamin by dynasore and inhibition of dynamin expression by siRNA resulted in a reduction in basolateral to apical transcytosis of EBV. Inhibition of Rac-1 and Cdc42, which are critical for macropinocytosis, also reduced EBV basolateral to apical transcytosis. It has been shown that Rac-1 may play role in internalization of E-cadherin via caveolin-associated endocytosis (117). Activation of Rac-1 is directly associated with lipid rafts, and although Cdc42 is not directly associated with lipid rafts, it is readily activated by raft-associated moieties (118). It is possible that Rac-1 and Cdc42 might be involved in caveolin-mediated endocytosis of EBV from basolateral membranes of polarized cells.

Cholesterol-containing lipid rafts play an important role in EBV entry into B lymphocytes (119), which occurs by endocytosis (9, 10). Interestingly, EBV entry into nonpolarized epithelial cells was found to be mediated by direct fusion of viral and cellular membranes (9, 10). We cannot exclude the possibility of EBV entry into polarized cells by direct viral fusion. Although we did not specifically investigate this process in the present work, viral fusion would not lead to transcytosis of uncoated virions through polarized epithelial cells.

It has been well documented that continuous EBV shedding into saliva occurs in EBV-seropositive individuals (29, 120). Thus, EBV-infected intraepithelial B lymphocytes and epithelial cells may produce viral particles, which may migrate through uninfected oral epithelial cells by basolateral to apical transcytosis, leading to shedding of virions into saliva.

EBV-specific sera reduced EBV apical to basolateral and basolateral to apical transcytosis; however, inhibition of basolateral to apical transcytosis was much stronger than inhibition of apical to basolateral transcytosis. These findings suggest that EBV glycoproteins may not play major roles in viral macropinocytosis from the apical surface of tonsil epithelial cells and that other mechanisms could be involved in this process. It has been reported that tonsil epithelium expresses the Fc receptor FCγIII (121), which may facilitate apical to basolateral transcytosis of IgG-coated EBV virions. A similar mechanism has been shown for HCMV: the neonatal Fc receptor facilitates apical to basolateral transcytosis of IgG-coated HCMV in placental epithelial cells (56). Importantly, transcytosed HCMV virions bound with nonneutralizing and low-neutralizing antibodies retained their infectivity. The majority of EBV virions in saliva are coated with antibodies (122); thus, virion-bound IgG may play a role in EBV apical to basolateral transcytosis. It is also possible that EBV envelope-associated phospholipids may trigger macropinocytosis of IgG-uncoated virions, as has been shown for other viral pathogens, including vaccinia and influenza viruses (93, 95, 123). We anticipate that future studies will better define the roles of Fc receptors and EBV phospholipids in viral apical to basolateral transcytosis. Strong inhibition of basolateral to apical transcytosis by EBV-specific sera supports the notion that viral envelope glycoproteins could be involved in the initiation of caveolin-mediated endocytosis, which is a receptor ligand-dependent process.

We previously showed that the EBV glycoprotein BMRF-2 binds to basolaterally sorted β1 and α5β1 integrins and facilitates EBV entry from basolateral membranes of polarized oral epithelial cells, leading to productive infection (18, 21). Here we show that EBV entry from basolateral membranes may also initiate transcytosis of virions through polarized oral epithelial cells long before the establishment of productive infection, i.e., 2 to 4 h after attachment of virions to basolateral membranes. It is possible that BMRF-2-mediated EBV entry may feed into two separate pathways of intracellular transport, with EBV entry from basolateral membranes leading to (i) delivery of virions to nuclei with initiation of productive infection and (ii) transcytosis of virions to apical membranes. It is well known that integrins are constitutively endocytosed and that β1 integrin (including α5β1) endocytosis is predominantly caveolin dependent (124–127), which is consistent with caveolin-dependent EBV endocytosis and transcytosis at basolateral membranes of oral epithelial cells. Further study may elucidate the functional role of BMRF-2 in this process.

EBV gHgL also binds to αvβ5, αvβ6, and αvβ8 integrins, and this binding triggers fusion of viral membranes with cell membranes, leading to productive infection (11, 12). As most integrins are sorted to the basolateral membranes of polarized epithelial cells, gHgL-mediated virus entry may also occur from basolateral membranes of oral epithelial cells. We showed approximately 90% inhibition of viral entry by cholesterol depletion. Since herpesvirus fusion may be influenced by the lipid composition of membranes (128, 129), cholesterol depletion may also lead to a reduction in virus fusion. Accordingly, we cannot rule out gHgL-mediated EBV basolateral entry by direct fusion of viral envelopes with cell membranes. The approximately 90% inhibition of EBV basolateral entry by cholesterol depletion may include inhibition of both viral endocytosis and direct viral fusion.

In summary, oral mucosal epithelial cells have a polarized organization that facilitates EBV transcytosis from apical to basolateral and from basolateral to apical membranes. EBV transcellular migration from the apical surfaces of epithelial cells to their basolateral membranes was found to be initiated by macropinocytosis. EBV apical to basolateral transcytosis across oral mucosal epithelium may facilitate delivery of virions to subepithelial B lymphocytes and serve as a key mechanism for primary EBV infection. EBV basolateral to apical transcytosis occurs through formation of caveolae and caveosomal vesicles and leads to secretion of viral progeny from the epithelium into saliva in EBV-infected individuals. Identification of the cellular targets for EBV transcytosis may lead to a better understanding of the biology of EBV infection of oral mucosa, including the molecular mechanisms of initial viral infection and secretion of virus into saliva in EBV-seropositive individuals. Furthermore, specific inactivation of EBV-induced macropinocytosis could be useful for preventing EBV infection in vulnerable risk groups, such as EBV-negative transplant recipients.

ACKNOWLEDGMENTS

We thank Larry Ackerman (University of California San Francisco, Diabetes Center Microscopy Core) for electron microscopy and Matthew Petitt for editorial assistance.

This project was supported by National Institutes of Health grants R01 DE14894, R21 DE016009, and R21 DE021011 and the UCSF ARI Carl L. Gaylord Estate fund and UCSF CFAR grant (to S.M.T.).

REFERENCES

1. **Rickinson AB, Kieff E.** 2001. Epstein-Barr virus, p 2575–2627. *In* Knipe DM, Howley PM, Griffin DE, Lamb RA, Martin MA, Roizman B, Straus SE (ed), Fields virology, 4th ed, vol 2. Lippincott Williams & Wilkins, Philadelphia, PA.
2. **Hutt-Fletcher LM.** 2007. Epstein-Barr virus entry. J. Virol. **81:**7825–7832.
3. **Spear PG, Longnecker R.** 2003. Herpesvirus entry: an update. J. Virol. **77:**10179–10185.
4. **Haan KM, Lee SK, Longnecker R.** 2001. Different functional domains in the cytoplasmic tail of glycoprotein B are involved in Epstein-Barr virus-induced membrane fusion. Virology **290:**106–114.
5. **Li Q, Spriggs MK, Kovats S, Turk SM, Comeau MR, Nepom B, Hutt-Fletcher LM.** 1997. Epstein-Barr virus uses HLA class II as a cofactor for infection of B lymphocytes. J. Virol. **71:**4657–4662.
6. **Li Q, Turk SM, Hutt-Fletcher LM.** 1995. The Epstein-Barr virus (EBV) BZLF2 gene product associates with the gH and gL homologs of EBV and carries an epitope critical to infection of B cells but not of epithelial cells. J. Virol. **69:**3987–3994.
7. **Sorem J, Jardetzky TS, Longnecker R.** 2009. Cleavage and secretion of Epstein-Barr virus glycoprotein 42 promote membrane fusion with B lymphocytes. J. Virol. **83:**6664–6672.
8. **Sorem J, Longnecker R.** 2009. Cleavage of Epstein-Barr virus glycoprotein B is required for full function in cell-cell fusion with both epithelial and B cells. J. Gen. Virol. **90:**591–595.
9. **Borza CM, Morgan AJ, Turk SM, Hutt-Fletcher LM.** 2004. Use of gHgL for attachment of Epstein-Barr virus to epithelial cells compromises infection. J. Virol. **78:**5007–5014.
10. **Miller N, Hutt-Fletcher LM.** 1992. Epstein-Barr virus enters B cells and epithelial cells by different routes. J. Virol. **66:**3409–3414.
11. **Chesnokova LS, Hutt-Fletcher LM.** 2011. Fusion of Epstein-Barr virus with epithelial cells can be triggered by alphavbeta5 in addition to alphavbeta6 and alphavbeta8, and integrin binding triggers a conformational change in glycoproteins gHgL. J. Virol. **85:**13214–13223.
12. **Chesnokova LS, Nishimura SL, Hutt-Fletcher LM.** 2009. Fusion of epithelial cells by Epstein-Barr virus proteins is triggered by binding of viral glycoproteins gHgL to integrins alphavbeta6 or alphavbeta8. Proc. Natl. Acad. Sci. U. S. A. **106:**20464–20469.
13. **McShane MP, Longnecker R.** 2004. Cell-surface expression of a mutated Epstein-Barr virus glycoprotein B allows fusion independent of other viral proteins. Proc. Natl. Acad. Sci. U. S. A. **101:**17474–17479.
14. **Molesworth SJ, Lake CM, Borza CM, Turk SM, Hutt-Fletcher LM.** 2000. Epstein-Barr virus gH is essential for penetration of B cells but also plays a role in attachment of virus to epithelial cells. J. Virol. **74:**6324–6332.
15. **Omerović J, Lev L, Longnecker R.** 2005. The amino terminus of Epstein-Barr virus glycoprotein gH is important for fusion with epithelial and B cells. J. Virol. **79:**12408–12415.
16. **Plate AE, Smajlovic J, Jardetzky TS, Longnecker R.** 2009. Functional analysis of glycoprotein L (gL) from rhesus lymphocryptovirus in Epstein-Barr virus-mediated cell fusion indicates a direct role of gL in gB-induced membrane fusion. J. Virol. **83:**7678–7689.
17. **Spear PG.** 1993. Membrane fusion induced by herpes simplex virus, p 201–232. *In* Bentz J (ed), Viral fusion mechanisms. CRC Press, Boca Raton, FL.
18. **Tugizov SM, Berline JW, Palefsky JM.** 2003. Epstein-Barr virus infection of polarized tongue and nasopharyngeal epithelial cells. Nat. Med. **9:**307–314.
19. **Xiao J, Palefsky JM, Herrera R, Berline J, Tugizov SM.** 2009. EBV BMRF-2 facilitates cell-to-cell spread of virus within polarized oral epithelial cells. Virology **388:**335–343.
20. **Xiao J, Palefsky JM, Herrera R, Berline J, Tugizov SM.** 2008. The Epstein-Barr virus BMRF-2 protein facilitates virus attachment to oral epithelial cells. Virology **370:**430–442.
21. **Xiao J, Palefsky JM, Herrera R, Tugizov SM.** 2007. Characterization of the Epstein-Barr virus glycoprotein BMRF-2. Virology **359:**382–396.
22. **Lemon SM, Hutt LM, Shaw JE, Li JL, Pagano JS.** 1977. Replication of EBV in epithelial cells during infectious mononucleosis. Nature **268:**268–270.
23. **Niedobitek G, Young LS, Lau R, Brooks L, Greenspan D, Greenspan JS, Rickinson AB.** 1991. Epstein-Barr virus infection in oral hairy leukoplakia: virus replication in the absence of a detectable latent phase. J. Gen. Virol. **72:**3035–3046.
24. **Pegtel DM, Middeldorp J, Thorley-Lawson DA.** 2004. Epstein-Barr virus infection in ex vivo tonsil epithelial cell cultures of asymptomatic carriers. J. Virol. **78:**12613–12624.
25. **Rickinson A.** 1984. Epstein-Barr virus in epithelium. Nature **310:**99–100.
26. **Sixbey JW, Nedrud JG, Raab-Traub N, Hanes RA, Pagano JS.** 1984. Epstein-Barr virus replication in oropharyngeal epithelial cells. N. Engl. J. Med. **310:**1225–1230.
27. **Young LS, Dawson CW, Clark D, Rupani H, Busson P, Tursz T, Johnson A, Rickinson AB.** 1988. Epstein-Barr virus gene expression in nasopharyngeal carcinoma. J. Gen. Virol. **69**(Part 5):1051–1065.
28. **Dawson DR, III, Wang C, Danaher RJ, Lin Y, Kryscio RJ, Jacob RJ, Miller CS.** 2009. Salivary levels of Epstein-Barr virus DNA correlate with subgingival levels, not severity of periodontitis. Oral Dis. **15:**554–559.
29. **Hadinoto V, Shapiro M, Sun CC, Thorley-Lawson DA.** 2009. The dynamics of EBV shedding implicate a central role for epithelial cells in amplifying viral output. PLoS Pathog. **5:**e1000496. doi:10.1371/journal.ppat.1000496.
30. **Imbronito AV, Grande SR, Freitas NM, Okuda O, Lotufo RF, Nunes FD.** 2008. Detection of Epstein-Barr virus and human cytomegalovirus in blood and oral samples: comparison of three sampling methods. J. Oral Sci. **50:**25–31.
31. **Jacobson MA, Ditmer DP, Sinclair E, Martin JN, Deeks SG, Hunt P, Mocarski ES, Shiboski C.** 2009. Human herpesvirus replication and abnormal CD8+ T cell activation and low CD4+ T cell counts in antiretroviral-suppressed HIV-infected patients. PLoS One **4:**e5277. doi:10.1371/journal.pone.0005277.
32. **Jiang R, Scott RS, Hutt-Fletcher LM.** 2006. Epstein-Barr virus shed in saliva is high in B-cell-tropic glycoprotein gp42. J. Virol. **80:**7281–7283.
33. **Winning TA, Townsend GC.** 2000. Oral mucosal embryology and histology. Clin. Dermatol. **18:**499–511.
34. **Go M, Kojima T, Takano K, Murata M, Ichimiya S, Tsubota H, Himi T, Sawada N.** 2004. Expression and function of tight junctions in the crypt epithelium of human palatine tonsils. J. Histochem. Cytochem. **52:**1627–1638.
35. **Langbein L, Grund C, Kuhn C, Praetzel S, Kartenbeck J, Brandner JM, Moll I, Franke WW.** 2002. Tight junctions and compositionally related junctional structures in mammalian stratified epithelia and cell cultures derived therefrom. Eur. J. Cell Biol. **81:**419–435.
36. **Langbein L, Pape UF, Grund C, Kuhn C, Praetzel S, Moll I, Moll R, Franke WW.** 2003. Tight junction-related structures in the absence of a lumen: occludin, claudins and tight junction plaque proteins in densely packed cell formations of stratified epithelia and squamous cell carcinomas. Eur. J. Cell Biol. **82:**385–400.
37. **Takano K, Kojima T, Go M, Murata M, Ichimiya S, Himi T, Sawada N.** 2005. HLA-DR- and CD11c-positive dendritic cells penetrate beyond well-developed epithelial tight junctions in human nasal mucosa of allergic rhinitis. J. Histochem. Cytochem. **53:**611–619.
38. **Tugizov SM, Herrera R, Veluppillai P, Greenspan D, Soros V, Greene WC, Levy JA, Palefsky JM.** 2012. Differential transmission of HIV traversing fetal oral/intestinal epithelia and adult oral epithelia. J. Virol. **86:**2556–2570.
39. **Tugizov SM, Herrera R, Veluppillai P, Greenspan D, Soros V, Greene WC, Levy JA, Palefsky JM.** 2011. HIV is inactivated after transepithelial migration via adult oral epithelial cells but not fetal epithelial cells. Virology **409:**211–222.
40. **Bomsel M, Alfsen A.** 2003. Entry of viruses through the epithelial barrier: pathogenic trickery. Nat. Rev. Mol. Cell Biol. **4:**57–68.
41. **Compans RW.** 1995. Virus entry and release in polarized epithelial cells. Curr. Top. Microbiol. Immunol. **202:**209–219.
42. **Mellman I.** 1996. Endocytosis and molecular sorting. Annu. Rev. Cell Dev. Biol. **12:**575–625.
43. **Mellman I.** 1995. Molecular sorting of membrane proteins in polarized and nonpolarized cells. Cold Spring Harbor Symp. Quant. Biol. **60:**745–752.
44. **Mostov KE, Verges M, Altschuler Y.** 2000. Membrane traffic in polarized epithelial cells. Curr. Opin. Cell Biol. **12:**483–490.
45. **Rodriguez-Boulan E, Powell SK.** 1992. Polarity of epithelial and neuronal cells. Annu. Rev. Cell Biol. **8:**395–427.
46. **Tucker SP, Compans RW.** 1993. Virus infection of polarized epithelial cells. Adv. Virus Res. **42:**187–247.

47. **Tugizov S, Maidji E, Pereira L.** 1996. Role of apical and basolateral membranes in replication of human cytomegalovirus in polarized retinal pigment epithelial cells. J. Gen. Virol. **77:**61–74.
48. **Tugizov S, Maidji E, Xiao J, Zheng Z, Pereira L.** 1998. Human cytomegalovirus glycoprotein B contains autonomous determinants for vectorial targeting to apical membranes of polarized epithelial cells. J. Virol. **72:**7374–7386.
49. **Shannon-Lowe C, Rowe M.** 2011. Epstein-Barr virus infection of polarized epithelial cells via the basolateral surface by memory B cell-mediated transfer infection. PLoS Pathog. **7:**e1001338. doi:10.1371/journal.ppat.1001338.
50. **Tugizov S, Herrera R, Veluppillai P, Greenspan J, Greenspan D, Palefsky JM.** 2007. Epstein-Barr virus (EBV)-infected monocytes facilitate dissemination of EBV within the oral mucosal epithelium. J. Virol. **81:**5484–5496.
51. **Bobardt MD, Chatterji U, Selvarajah S, Van der Schueren B, David G, Kahn B, Gallay PA.** 2007. Cell-free human immunodeficiency virus type 1 transcytosis through primary genital epithelial cells. J. Virol. **81:**395–405.
52. **Bomsel M.** 1997. Transcytosis of infectious human immunodeficiency virus across a tight human epithelial cell line barrier. Nat. Med. **3:**42–47.
53. **Chodosh J, Gan Y, Holder VP, Sixbey JW.** 2000. Patterned entry and egress by Epstein-Barr virus in polarized CR2-positive epithelial cells. Virology **266:**387–396.
54. **Fujimura Y, Takeda M, Ikai H, Haruma K, Akisada T, Harada T, Sakai T, Ohuchi M.** 2004. The role of M cells of human nasopharyngeal lymphoid tissue in influenza virus sampling. Virchows Arch. **444:**36–42.
55. **Hocini H, Bomsel M.** 1999. Infectious human immunodeficiency virus can rapidly penetrate a tight human epithelial barrier by transcytosis in a process impaired by mucosal immunoglobulins. J. Infect. Dis. **179**(Suppl 3):S448–S453.
56. **Maidji E, McDonagh S, Genbacev O, Tabata T, Pereira L.** 2006. Maternal antibodies enhance or prevent cytomegalovirus infection in the placenta by neonatal Fc receptor-mediated transcytosis. Am. J. Pathol. **168:**1210–1226.
57. **Meng G, Wei X, Wu X, Sellers MT, Decker JM, Moldoveanu Z, Orenstein JM, Graham MF, Kappes JC, Mestecky J, Shaw GM, Smith PD.** 2002. Primary intestinal epithelial cells selectively transfer R5 HIV-1 to CCR5+ cells. Nat. Med. **8:**150–156.
58. **Ouzilou L, Caliot E, Pelletier I, Prevost MC, Pringault E, Colbere-Garapin F.** 2002. Poliovirus transcytosis through M-like cells. J. Gen. Virol. **83:**2177–2182.
59. **Saïdi H, Magri G, Nasreddine N, Requena M, Belec L.** 2007. R5- and X4-HIV-1 use differentially the endometrial epithelial cells HEC-1A to ensure their own spread: implication for mechanisms of sexual transmission. Virology **358:**55–68.
60. **Tuma PL, Hubbard AL.** 2003. Transcytosis: crossing cellular barriers. Physiol. Rev. **83:**871–932.
61. **Gulino D, Delachanal E, Concord E, Genoux Y, Morand B, Valiron MO, Sulpice E, Scaife R, Alemany M, Vernet T.** 1998. Alteration of endothelial cell monolayer integrity triggers resynthesis of vascular endothelium cadherin. J. Biol. Chem. **273:**29786–29793.
62. **Takada K.** 1984. Cross-linking of cell surface immunoglobulins induces Epstein-Barr virus in Burkitt lymphoma lines. Int. J. Cancer **33:**27–32.
63. **Geiser V, Cahir-McFarland E, Kieff E.** 2011. Latent membrane protein 1 is dispensable for Epstein-Barr virus replication in human embryonic kidney 293 cells. PLoS One **6:**e22929. doi:10.1371/journal.pone.0022929.
64. **Qin Z, Freitas E, Sullivan R, Mohan S, Bacelieri R, Branch D, Romano M, Kearney P, Oates J, Plaisance K, Renne R, Kaleeba J, Parsons C.** 2010. Upregulation of xCT by KSHV-encoded microRNAs facilitates KSHV dissemination and persistence in an environment of oxidative stress. PLoS Pathog. **6:**e1000742. doi:10.1371/journal.ppat.1000742.
65. **Sandgren KJ, Wilkinson J, Miranda-Saksena M, McInerney GM, Byth-Wilson K, Robinson PJ, Cunningham AL.** 2010. A differential role for macropinocytosis in mediating entry of the two forms of vaccinia virus into dendritic cells. PLoS Pathog. **6:**e1000866. doi:10.1371/journal.ppat.1000866.
66. **Xiao J, Palefsky JM, Herrera R, Sunshine C, Tugizov SM.** 2009. EBV-positive human sera contain antibodies against the EBV BMRF-2 protein. Virology **393:**151–159.
67. **Francis SA, Kelly JM, McCormack J, Rogers RA, Lai J, Schneeberger EE, Lynch RD.** 1999. Rapid reduction of MDCK cell cholesterol by methyl-beta-cyclodextrin alters steady state transepithelial electrical resistance. Eur. J. Cell Biol. **78:**473–484.
68. **Kamioka N, Akahane T, Kohno Y, Kuroki T, Iijima M, Honma I, Ohba M.** 2010. Protein kinase C delta and eta differently regulate the expression of loricrin and Jun family proteins in human keratinocytes. Biochem. Biophys. Res. Commun. **394:**106–111.
69. **Ryan JL, Fan H, Glaser SL, Schichman SA, Raab-Traub N, Gulley ML.** 2004. Epstein-Barr virus quantitation by real-time PCR targeting multiple gene segments: a novel approach to screen for the virus in paraffin-embedded tissue and plasma. J. Mol. Diagn. **6:**378–385.
70. **Steinau M, Rajeevan MS, Unger ER.** 2006. DNA and RNA references for qRT-PCR assays in exfoliated cervical cells. J. Mol. Diagn. **8:**113–118.
71. **Halder S, Murakami M, Verma SC, Kumar P, Yi F, Robertson ES.** 2009. Early events associated with infection of Epstein-Barr virus infection of primary B-cells. PLoS One **4:**e7214. doi:10.1371/journal.pone.0007214.
72. **Livak KJ, Schmittgen TD.** 2001. Analysis of relative gene expression data using real-time quantitative PCR and the 2(−Delta Delta C(T)) method. Methods **25:**402–408.
73. **Rescigno M, Urbano M, Valzasina B, Francolini M, Rotta G, Bonasio R, Granucci F, Kraehenbuhl JP, Ricciardi-Castagnoli P.** 2001. Dendritic cells express tight junction proteins and penetrate gut epithelial monolayers to sample bacteria. Nat. Immunol. **2:**361–367.
74. **Krautkrämer E, Zeier M.** 2008. Hantavirus causing hemorrhagic fever with renal syndrome enters from the apical surface and requires decay-accelerating factor (DAF/CD55). J. Virol. **82:**4257–4264.
75. **Ivanov AI.** 2008. Pharmacological inhibition of endocytic pathways: is it specific enough to be useful? Methods Mol. Biol. **440:**15–33.
76. **Ivanov AI, Nusrat A, Parkos CA.** 2004. Endocytosis of epithelial apical junctional proteins by a clathrin-mediated pathway into a unique storage compartment. Mol. Biol. Cell **15:**176–188.
77. **Spoden G, Freitag K, Husmann M, Boller K, Sapp M, Lambert C, Florin L.** 2008. Clathrin- and caveolin-independent entry of human papillomavirus type 16—involvement of tetraspanin-enriched microdomains (TEMs). PLoS One **3:**e3313. doi:10.1371/journal.pone.0003313.
78. **Vercauteren D, Vandenbroucke RE, Jones AT, Rejman J, Demeester J, De Smedt SC, Sanders NN, Braeckmans K.** 2010. The use of inhibitors to study endocytic pathways of gene carriers: optimization and pitfalls. Mol. Ther. **18:**561–569.
79. **Saeed MF, Kolokoltsov AA, Albrecht T, Davey RA.** 2010. Cellular entry of Ebola virus involves uptake by a macropinocytosis-like mechanism and subsequent trafficking through early and late endosomes. PLoS Pathog. **6:**e1001110. doi:10.1371/journal.ppat.1001110.
80. **Hewlett LJ, Prescott AR, Watts C.** 1994. The coated pit and macropinocytic pathways serve distinct endosome populations. J. Cell Biol. **124:**689–703.
81. **Kerr MC, Lindsay MR, Luetterforst R, Hamilton N, Simpson F, Parton RG, Gleeson PA, Teasdale RD.** 2006. Visualisation of macropinosome maturation by the recruitment of sorting nexins. J. Cell Sci. **119:**3967–3980.
82. **Swanson JA, Watts C.** 1995. Macropinocytosis. Trends Cell Biol. **5:**424–428.
83. **Haspot F, Lavault A, Sinzger C, Laib Sampaio K, Stierhof YD, Pilet P, Bressolette-Bodin C, Halary F.** 2012. Human cytomegalovirus entry into dendritic cells occurs via a macropinocytosis-like pathway in a pH-independent and cholesterol-dependent manner. PLoS One **7:**e34795. doi:10.1371/journal.pone.0034795.
84. **Maréchal V, Prevost MC, Petit C, Perret E, Heard JM, Schwartz O.** 2001. Human immunodeficiency virus type 1 entry into macrophages mediated by macropinocytosis. J. Virol. **75:**11166–11177.
85. **Raghu H, Sharma-Walia N, Veettil MV, Sadagopan S, Chandran B.** 2009. Kaposi's sarcoma-associated herpesvirus utilizes an actin polymerization-dependent macropinocytic pathway to enter human dermal microvascular endothelial and human umbilical vein endothelial cells. J. Virol. **83:**4895–4911.
86. **Rossman JS, Leser GP, Lamb RA.** 2012. Filamentous influenza virus enters cells via macropinocytosis. J. Virol. **86:**10950–10960.
87. **Sánchez EG, Quintas A, Perez-Nunez D, Nogal M, Barroso S, Carrascosa AL, Revilla Y.** 2012. African swine fever virus uses macropinocytosis to enter host cells. PLoS Pathog. **8:**e1002754. doi:10.1371/journal.ppat.1002754.
88. **Fadok VA, Bratton DL, Frasch SC, Warner ML, Henson PM.** 1998.

The role of phosphatidylserine in recognition of apoptotic cells by phagocytes. Cell Death Differ. **5:**551–562.
89. **Fadok VA, Bratton DL, Rose DM, Pearson A, Ezekewitz RA, Henson PM.** 2000. A receptor for phosphatidylserine-specific clearance of apoptotic cells. Nature **405:**85–90.
90. **Fadok VA, Henson PM.** 2003. Apoptosis: giving phosphatidylserine recognition an assist—with a twist. Curr. Biol. **13:**R655–R657.
91. **Fadok VA, Xue D, Henson P.** 2001. If phosphatidylserine is the death knell, a new phosphatidylserine-specific receptor is the bellringer. Cell Death Differ. **8:**582–587.
92. **Mercer J, Helenius A.** 2010. Apoptotic mimicry: phosphatidylserine-mediated macropinocytosis of vaccinia virus. Ann. N. Y. Acad. Sci. **1209:** 49–55.
93. **Mercer J, Helenius A.** 2008. Vaccinia virus uses macropinocytosis and apoptotic mimicry to enter host cells. Science **320:**531–535.
94. **Mercer J, Helenius A.** 2009. Virus entry by macropinocytosis. Nat. Cell Biol. **11:**510–520.
95. **Mercer J, Knebel S, Schmidt FI, Crouse J, Burkard C, Helenius A.** 2010. Vaccinia virus strains use distinct forms of macropinocytosis for host-cell entry. Proc. Natl. Acad. Sci. U. S. A. **107:**9346–9351.
96. **Vogel U, Sandvig K, van Deurs B.** 1998. Expression of caveolin-1 and polarized formation of invaginated caveolae in Caco-2 and MDCK II cells. J. Cell Sci. **111**(Part 6):825–832.
97. **Breton S, Lisanti MP, Tyszkowski R, McLaughlin M, Brown D.** 1998. Basolateral distribution of caveolin-1 in the kidney. Absence from H+-atpase-coated endocytic vesicles in intercalated cells. J. Histochem. Cytochem. **46:**205–214.
98. **Manninen A, Verkade P, Le Lay S, Torkko J, Kasper M, Fullekrug J, Simons K.** 2005. Caveolin-1 is not essential for biosynthetic apical membrane transport. Mol. Cell. Biol. **25:**10087–10096.
99. **Frank PG, Cheung MW, Pavlides S, Llaverias G, Park DS, Lisanti MP.** 2006. Caveolin-1 and regulation of cellular cholesterol homeostasis. Am. J. Physiol. Heart Circ. Physiol. **291:**H677–H686.
100. **Sharma DK, Brown JC, Choudhury A, Peterson TE, Holicky E, Marks DL, Simari R, Parton RG, Pagano RE.** 2004. Selective stimulation of caveolar endocytosis by glycosphingolipids and cholesterol. Mol. Biol. Cell **15:**3114–3122.
101. **Amstutz B, Gastaldelli M, Kalin S, Imelli N, Boucke K, Wandeler E, Mercer J, Hemmi S, Greber UF.** 2008. Subversion of CtBP1-controlled macropinocytosis by human adenovirus serotype 3. EMBO J. **27:**956–969.
102. **Chakraborty S, ValiyaVeettil M, Sadagopan S, Paudel N, Chandran B.** 2011. c-Cbl-mediated selective virus-receptor translocations into lipid rafts regulate productive Kaposi's sarcoma-associated herpesvirus infection in endothelial cells. J. Virol. **85:**12410–12430.
103. **Coyne CB, Shen L, Turner JR, Bergelson JM.** 2007. Coxsackievirus entry across epithelial tight junctions requires occludin and the small GTPases Rab34 and Rab5. Cell Host Microbe **2:**181–192.
104. **Liu NQ, Lossinsky AS, Popik W, Li X, Gujuluva C, Kriederman B, Roberts J, Pushkarsky T, Bukrinsky M, Witte M, Weinand M, Fiala M.** 2002. Human immunodeficiency virus type 1 enters brain microvascular endothelia by macropinocytosis dependent on lipid rafts and the mitogen-activated protein kinase signaling pathway. J. Virol. **76:**6689–6700.
105. **Meier O, Boucke K, Hammer SV, Keller S, Stidwill RP, Hemmi S, Greber UF.** 2002. Adenovirus triggers macropinocytosis and endosomal leakage together with its clathrin-mediated uptake. J. Cell Biol. **158:** 1119–1131.
106. **Mulherkar N, Raaben M, de la Torre JC, Whelan SP, Chandran K.** 2011. The Ebola virus glycoprotein mediates entry via a non-classical dynamin-dependent macropinocytic pathway. Virology **419:**72–83.
107. **Pernet O, Pohl C, Ainouze M, Kweder H, Buckland R.** 2009. Nipah virus entry can occur by macropinocytosis. Virology **395:**298–311.
108. **Schelhaas M.** 2010. Come in and take your coat off—how host cells provide endocytosis for virus entry. Cell. Microbiol. **12:**1378–1388.
109. **Valiya Veettil M, Sadagopan S, Kerur N, Chakraborty S, Chandran B.** 2010. Interaction of c-Cbl with myosin IIA regulates Bleb associated macropinocytosis of Kaposi's sarcoma-associated herpesvirus. PLoS Pathog. **6:**e1001238. doi:10.1371/journal.ppat.1001238.
110. **Van den Broeke C, Radu M, Chernoff J, Favoreel HW.** 2010. An emerging role for p21-activated kinases (Paks) in viral infections. Trends Cell Biol. **20:**160–169.
111. **Liu YW, Surka MC, Schroeter T, Lukiyanchuk V, Schmid SL.** 2008. Isoform and splice-variant specific functions of dynamin-2 revealed by analysis of conditional knock-out cells. Mol. Biol. Cell **19:**5347–5359.
112. **Schlunck G, Damke H, Kiosses WB, Rusk N, Symons MH, Waterman-Storer CM, Schmid SL, Schwartz MA.** 2004. Modulation of Rac localization and function by dynamin. Mol. Biol. Cell **15:**256–267.
113. **Harder CJ, Meng A, Rippstein P, McBride HM, McPherson R.** 2007. SR-BI undergoes cholesterol-stimulated transcytosis to the bile canaliculus in polarized WIF-B cells. J. Biol. Chem. **282:**1445–1455.
114. **Leyt J, Melamed-Book N, Vaerman JP, Cohen S, Weiss AM, Aroeti B.** 2007. Cholesterol-sensitive modulation of transcytosis. Mol. Biol. Cell **18:**2057–2071.
115. **Lajoie P, Kojic LD, Nim S, Li L, Dennis JW, Nabi IR.** 2009. Caveolin-1 regulation of dynamin-dependent, raft-mediated endocytosis of cholera toxin-B sub-unit occurs independently of caveolae. J. Cell. Mol. Med. **13:**3218–3225.
116. **Nabi IR, Le PU.** 2003. Caveolae/raft-dependent endocytosis. J. Cell Biol. **161:**673–677.
117. **Akhtar N, Hotchin NA.** 2001. RAC1 regulates adherens junctions through endocytosis of E-cadherin. Mol. Biol. Cell **12:**847–862.
118. **Jaksits S, Bauer W, Kriehuber E, Zeyda M, Stulnig TM, Stingl G, Fiebiger E, Maurer D.** 2004. Lipid raft-associated GTPase signaling controls morphology and CD8+ T cell stimulatory capacity of human dendritic cells. J. Immunol. **173:**1628–1639.
119. **Katzman RB, Longnecker R.** 2003. Cholesterol-dependent infection of Burkitt's lymphoma cell lines by Epstein-Barr virus. J. Gen. Virol. **84:** 2987–2992.
120. **Ikuta K, Satoh Y, Hoshikawa Y, Sairenji T.** 2000. Detection of Epstein-Barr virus in salivas and throat washings in healthy adults and children. Microbes Infect. **2:**115–120.
121. **Moutsopoulos NM, Nares S, Nikitakis N, Rangel Z, Wen J, Munson P, Sauk J, Wahl SM.** 2007. Tonsil epithelial factors may influence oropharyngeal human immunodeficiency virus transmission. Am. J. Pathol. **171:**571–579.
122. **Turk SM, Jiang R, Chesnokova LS, Hutt-Fletcher LM.** 2006. Antibodies to gp350/220 enhance the ability of Epstein-Barr virus to infect epithelial cells. J. Virol. **80:**9628–9633.
123. **Shiratsuchi A, Kaido M, Takizawa T, Nakanishi Y.** 2000. Phosphatidylserine-mediated phagocytosis of influenza A virus-infected cells by mouse peritoneal macrophages. J. Virol. **74:**9240–9244.
124. **Bretscher MS.** 1992. Circulating integrins: alpha 5 beta 1, alpha 6 beta 4 and Mac-1, but not alpha 3 beta 1, alpha 4 beta 1 or LFA-1. EMBO J. **11:**405–410.
125. **Bretscher MS.** 1989. Endocytosis and recycling of the fibronectin receptor in CHO cells. EMBO J. **8:**1341–1348.
126. **Pellinen T, Ivaska J.** 2006. Integrin traffic. J. Cell Sci. **119:**3723–3731.
127. **Shi F, Sottile J.** 2008. Caveolin-1-dependent beta1 integrin endocytosis is a critical regulator of fibronectin turnover. J. Cell Sci. **121:**2360–2371.
128. **Falanga A, Tarallo R, Vitiello G, Vitiello M, Perillo E, Cantisani M, D'Errico G, Galdiero M, Galdiero S.** 2012. Biophysical characterization and membrane interaction of the two fusion loops of glycoprotein B from herpes simplex type I virus. PLoS One **7:**e32186. doi:10.1371/journal.pone.0032186.
129. **Rahn E, Petermann P, Hsu MJ, Rixon FJ, Knebel-Morsdorf D.** 2011. Entry pathways of herpes simplex virus type 1 into human keratinocytes are dynamin- and cholesterol-dependent. PLoS One **6:**e25464. doi:10.1371/journal.pone.0025464.